$V_{max}{}^{app}$ and $K_m{}^{app}$ are defined as

$$V_{\max}{}^{app} = k_{cat}{}^{app}[E] \quad (2)$$

and

$$K_m{}^{app} = K_m \frac{(1+\frac{[I]}{K_i})}{(1+\frac{[I]}{K_i'})}, \quad (3)$$

respectively, where K_m is the Michaelis-Menten constant; $[E]$ is the enzyme concentration; $[I]$ is the inhibitor concentration; K_i and K_i' are the inhibition constants for the enzyme and the complex of the enzyme with substrate; and $k_{cat}{}^{app}$ is the apparent turnover number:

$$k_{cat}{}^{app} = \frac{k_{cat}}{(1+\frac{[I]}{K_i'})}, \quad (4)$$

where k_{cat} is the turnover number.

The $k_{cat}{}^{app}$ and $K_m{}^{app}$ that can be derived from the model (Figure 2C) are

$$k_{cat}{}^{app} = \frac{k_{cat}}{(1+\frac{[I^{ATP}]}{K_i'^{ATP}})} \quad (5)$$

and

$$K_m{}^{app} = \frac{K_m(1+\frac{[I^{ATP}]}{K_i^{ATP}}+\frac{[I^{AZT}]}{K_i^{AZT}}+\frac{[I^{AZT}][I^{ATP}]}{K_i''^{ATP}K_i^{AZT}})}{(1+\frac{[I^{ATP}]}{K_i'^{ATP}})}, \quad (6)$$

where K_i^{ATP} is the dissociation constant of ATP; K_i^{AZTTP} is the dissociation constant of AZTTP; $[I^{ATP}]$ is the ATP concentration; and $[I^{AZTTP}]$ is the AZTTP concentration.

Structural Analysis

We constructed the 3-D models of HIV-1 RTs by homology modeling [19] using the Molecular Operating Environment, MOE (Chemical Computing Group, Canada) as previously described [34]. We generated models of the 93JPNH-1 RT and ERT-mt6 RT structures at the pre- and post-translocation stages, which theoretically are competent for the binding of the incoming-ATP. We used two crystal structures of the HIV-1 RTs (PDB code: 1N6Q [14] and 1RTD [1]) as modeling templates. The sequence identities of the 1N6Q and 1RTD with the 93JPNH-1 RT and ERT-mt6 RT are ~90%. We optimized the 3-D structure thermodynamically by energy minimization using MOE and an AMBER94 force field. We further refined the physically unacceptable local structure of the models on the basis of evaluation by the Ramachandran plot using MOE. The optimized models were docked with ATP with the automated ligand docking program ASEDock2005 [22] (Ryoka Systems, Japan) operated in the Molecular Operating Environment. The RT-template-primer-ATP complex structures were thermodynamically and sterically optimized as described above.

Site-Directed Mutagenesis

Site-directed mutagenesis was performed with a QuikChange Multi Site-Directed Mutagenesis Kit (Stratagene, USA), using pQE70 (Qiagen, Germany) containing the coding sequence of the p66 subunit of ERT-mt6 as the template. The positions of the amino acid substitutions corresponded to the positions 72, 110, 113, 116, and 219 of 93JP-NH1. The mutations and oligonucleotides used in the mutagenesis reaction were R72A (5′-CGGCCAGCA TTAAATGGgcGAAATTAGTAGATTTCAGAGAG-3′), R72Q (5′-CGGCCAGCATTAAATGGcaGAAATTAGTAGATTTCA-GAGAG-3′), D110A (5′-GAAAAAATCAGTAACAGTACTAG-cTGTGGGAGATGCATATTTTTC-3′), D110N (5′-GAAAAA-ATCAGTAACAGTACTAaATGTGGGAGATGCATATTTT-TC-3′), D113A (5′-CAGTACTAGATGTGGGAGcTGCATAT-TTTTCAGTTCCTT-3′), D113N (5′-CAGTACTAGATGTGG-GAaaTGCATATTTTTCAGTTCCTT-3′), F116A (5′-GGAA-CTGAAgcATATGCATCTCCCACATCTAGTACTG-3′), F116L (5′-GGAACTGAcAAATATGCATCTCCCACATCTAGTACT-G-3′), K219A (5′-GGGATTTTATACACCAGACgcAAAGCAT-CAGAAGGAACCTC-3′), and K230(219)Q (5′-GGGATTTTA-TACACCAGACcAAAAGCATCAGAAGGAACCTC-3′), where the introduced mutations appear in lowercase letters. In all cases, the nucleotide sequences of the complete p66 coding region and of cloning sites were verified with an automated sequencer. The mutant p66 subunits were expressed in XL1-blue and used to form the p51/p66 heterodimer using the p51 subunit of 93JP-NH1 in binding buffer, as described above. The p51/p66 heterodimers were purified by Ni^{2+} affinity chromatography. About 104 to 221 μg of the p51/p66 heterodimers, with about 90% purity as judged by SDS-polyacrylamide gel electrophoresis (Figure S4A), were obtained from a 20 ml culture. The purified RTs were dissolved in the RT stock buffer and kept at −30°C until use.

Supporting Information

Figure S1 Data on RTs of 93JP-NH1 and ERT-mt6. A. Electrophoresis of the purified p51/p66 heterodimers of HIV-1 RTs. The purified p51/p66 heterodimers of 93JP-NH1 RT (NH1) and ERT-mt6 RT (mt6) were electrophoresed on an SDS-4/20% polyacrylamide gradient gel. The gel was stained with GelCode Blue Stain Reagent (Pierce, USA). (Lanes 1 and 4) Molecular size markers. B. The substrate-velocity curves of purified HIV-1 RTs. RNA-dependent DNA polymerase activity at the indicated concentrations of [α-^{32}P]dTTP was measured using purified RTs of 93JP-NH1 (1 nM) and ERT-mt6 (10 nM).
Found at: doi:10.1371/journal.pone.0008867.s001 (0.29 MB TIF)

Figure S2 Lineweaver-Burk double-reciprocal plots of AZTTP-dependent inhibition of dTTP incorporation. A. 93JP-NH1 RT. B. ERT-mt6. The initial velocities of dTMP incorporation into poly (rA)·p(dT)$_{12-18}$ were measured using [α-^{32}P]dTTP and purified RTs in the presence of AZTTP. Reciprocal values of the initial velocities and substrate concentrations are plotted.
Found at: doi:10.1371/journal.pone.0008867.s002 (0.15 MB TIF)

Figure S3 Docking simulations of ATP with RT-template-primer ternary complex models. A and C: 93JP-NH1 RT. B and D: ERT-mt6 RT. The 3-D models of the p66-template-primer complexes at the pre-translation stage (A and B) and the post-translation stage (C and D) were constructed by a homology modeling technique and docked with ATP using the ASEDock2005 (see Materials and Methods). Catalytic clefts composed of fingers, palm, and thumb subdomains are shown. ATP, red sticks; p66 main chain, grey ribbon; template-primer, grey sticks; motif A, blue ribbon.
Found at: doi:10.1371/journal.pone.0008867.s003 (1.93 MB TIF)

Figure S4 Data on RT mutants from the ERT-mt6 RT. A. Electrophoresis of the purified RT mutants from the ERT-mt6 RT. B. dTMP incorporations into poly (rA)·p(dT)$_{12-18}$ by the

mutant RTs. RNA-dependent DNA polymerase activity of the purified RTs (20 nM) was measured using a [α-^{32}P]dTTP and poly (rA)·p(dT)$_{12-18}$ system. C. Fold increases in the IC_{50} of AZTTP by ATP addition. IC_{50} values of AZTTP with RT mutants were calculated from the amounts of [α-^{32}P]dTTP incorporation in the presence of various concentrations (0–1 μM) of AZTTP and 5 mM ATP. Fold increases in IC_{50} compared to the values without ATP are shown. D. The substrate-velocity curves of purified HIV-1 RTs in the presence of ATP. RNA-dependent DNA polymerase activity of the purified mutant RTs was measured using various concentrations of [α-^{32}P]dTTP and poly (rA)·p(dT)$_{12-18}$ in the presence of ATP, Representative results with D113A RT (left) and K219A RT (right) are shown.
Found at: doi:10.1371/journal.pone.0008867.s004 (0.39 MB TIF)

Author Contributions

Conceived and designed the experiments: MY HS. Performed the experiments: MY HM. Analyzed the data: MY. Wrote the paper: MY HS.

References

1. Huang H, Chopra R, Verdine GL, Harrison SC (1998) Structure of a covalently trapped catalytic complex of HIV-1 reverse transcriptase: implications for drug resistance. Science 282: 1669–1675.
2. Preston BD, Poiesz BJ, Loeb LA (1988) Fidelity of HIV-1 reverse transcriptase. Science 242: 1168–1171.
3. Roberts JD, Bebenek K, Kunkel TA (1988) The accuracy of reverse transcriptase from HIV-1. Science 242: 1171–1173.
4. Goodman MF (1997) Hydrogen bonding revisited: geometric selection as a principal determinant of DNA replication fidelity. Proc Natl Acad Sci U S A 94: 10493–10495.
5. Kunkel TA, Bebenek K (2000) DNA replication fidelity. Annu Rev Biochem 69: 497–529.
6. Kunkel TA (2004) DNA replication fidelity. J Biol Chem 279: 16895–16898.
7. Traut TW (1994) Physiological concentrations of purines and pyrimidines. Mol Cell Biochem 140: 1–22.
8. Meyer PR, Matsuura SE, So AG, Scott WA (1998) Unblocking of chain-terminated primer by HIV-1 reverse transcriptase through a nucleotide-dependent mechanism. Proc Natl Acad Sci U S A 95: 13471–13476.
9. Arion D, Kaushik N, McCormick S, Borkow G, Parniak MA (1998) Phenotypic mechanism of HIV-1 resistance to 3′-azido-3′-deoxythymidine (AZT): increased polymerization processivity and enhanced sensitivity to pyrophosphate of the mutant viral reverse transcriptase. Biochemistry 37: 15908–15917.
10. Meyer PR, Matsuura SE, Mian AM, So AG, Scott WA (1999) A mechanism of AZT resistance: an increase in nucleotide-dependent primer unblocking by mutant HIV-1 reverse transcriptase. Mol Cell 4: 35–43.
11. Das K, Sarafianos SG, Clark AD Jr, Boyer PL, Hughes SH, et al. (2007) Crystal structures of clinically relevant Lys103Asn/Tyr181Cys double mutant HIV-1 reverse transcriptase in complexes with ATP and non-nucleoside inhibitor HBY 097. J Mol Biol 365: 77–89.
12. Sarafianos SG, Marchand B, Das K, Himmel DM, Parniak MA, et al. (2009) Structure and function of HIV-1 reverse transcriptase: molecular mechanisms of polymerization and inhibition. J Mol Biol 385: 693–713.
13. Sato H, Tomita Y, Ebisawa K, Hachiya A, Shibamura K, et al. (2001) Augmentation of human immunodeficiency virus type 1 subtype E (CRF01_AE) multiple-drug resistance by insertion of a foreign 11-amino-acid fragment into the reverse transcriptase. J Virol 75: 5604–5613.
14. Sarafianos SG, Clark AD Jr, Das K, Tuske S, Birktoft JJ, et al. (2002) Structures of HIV-1 reverse transcriptase with pre- and post-translocation AZTMP-terminated DNA. Embo J 21: 6614–6624.
15. Ray AS, Murakami E, Basavapathruni A, Vaccaro JA, Ulrich D, et al. (2003) Probing the molecular mechanisms of AZT drug resistance mediated by HIV-1 reverse transcriptase using a transient kinetic analysis. Biochemistry 42: 8831–8841.
16. Marchand B, White KL, Ly JK, Margot NA, Wang R, et al. (2007) Effects of the translocation status of human immunodeficiency virus type 1 reverse transcriptase on the efficiency of excision of tenofovir. Antimicrob Agents Chemother 51: 2911–2919.
17. Furman PA, Fyfe JA, St Clair MH, Weinhold K, Rideout JL, et al. (1986) Phosphorylation of 3′-azido-3′-deoxythymidine and selective interaction of the 5′-triphosphate with human immunodeficiency virus reverse transcriptase. Proc Natl Acad Sci U S A 83: 8333–8337.
18. Vrang L, Bazin H, Remaud G, Chattopadhyaya J, Oberg B (1987) Inhibition of the reverse transcriptase from HIV by 3′-azido-3′-deoxythymidine triphosphate and its threo analogue. Antiviral Res 7: 139–149.
19. Baker D, Sali A (2001) Protein structure prediction and structural genomics. Science 294: 93–96.
20. Kati WM, Johnson KA, Jerva LF, Anderson KS (1992) Mechanism and fidelity of HIV reverse transcriptase. J Biol Chem 267: 25988–25997.
21. Rittinger K, Divita G, Goody RS (1995) Human immunodeficiency virus reverse transcriptase substrate-induced conformational changes and the mechanism of inhibition by nonnucleoside inhibitors. Proc Natl Acad Sci U S A 92: 8046–8049.
22. Goto J, Kataoka R, Muta H, Hirayama N (2008) ASEDock-docking based on alpha spheres and excluded volumes. J Chem Inf Model 48: 583–590.
23. Chen R, Yokoyama M, Sato H, Reilly C, Mansky LM (2005) Human immunodeficiency virus mutagenesis during antiviral therapy: impact of drug-resistant reverse transcriptase and nucleoside and nonnucleoside reverse transcriptase inhibitors on human immunodeficiency virus type 1 mutation frequencies. J Virol 79: 12045–12057.
24. Li Y, Kong Y, Korolev S, Waksman G (1998) Crystal structures of the Klenow fragment of Thermus aquaticus DNA polymerase I complexed with deoxyribonucleoside triphosphates. Protein Sci 7: 1116–1123.
25. Johnson SJ, Taylor JS, Beese LS (2003) Processive DNA synthesis observed in a polymerase crystal suggests a mechanism for the prevention of frameshift mutations. Proc Natl Acad Sci U S A 100: 3895–3900.
26. Yin YW, Steitz TA (2004) The structural mechanism of translocation and helicase activity in T7 RNA polymerase. Cell 116: 393–404.
27. Temiakov D, Patlan V, Anikin M, McAllister WT, Yokoyama S, et al. (2004) Structural basis for substrate selection by t7 RNA polymerase. Cell 116: 381–391.
28. Thompson AA, Albertini RA, Peersen OB (2007) Stabilization of poliovirus polymerase by NTP binding and fingers-thumb interactions. J Mol Biol 366: 1459–1474.
29. Petruska J, Goodman MF, Boosalis MS, Sowers LC, Cheong C, et al. (1988) Comparison between DNA melting thermodynamics and DNA polymerase fidelity. Proc Natl Acad Sci U S A 85: 6252–6256.
30. Ling H, Boudsocq F, Woodgate R, Yang W (2001) Crystal structure of a Y-family DNA polymerase in action: a mechanism for error-prone and lesion-bypass replication. Cell 107: 91–102.
31. Ling H, Boudsocq F, Plosky BS, Woodgate R, Yang W (2003) Replication of a cis-syn thymine dimer at atomic resolution. Nature 424: 1083–1087.
32. Starnes MC, Cheng YC (1989) Human immunodeficiency virus reverse transcriptase-associated RNase H activity. J Biol Chem 264: 7073–7077.
33. Willey RL, Smith DH, Lasky LA, Theodore TS, Earl PL, et al. (1988) In vitro mutagenesis identifies a region within the envelope gene of the human immunodeficiency virus that is critical for infectivity. J Virol 62: 139–147.
34. Shirakawa K, Takaori-Kondo A, Yokoyama M, Izumi T, Matsui M, et al. (2008) Phosphorylation of APOBEC3G by protein kinase A regulates its interaction with HIV-1 Vif. Nat Struct Mol Biol 15: 1184–1191.

OPEN ACCESS Freely available online

PLoS one

Net Positive Charge of HIV-1 CRF01_AE V3 Sequence Regulates Viral Sensitivity to Humoral Immunity

Satoshi Naganawa[1,6☯], Masaru Yokoyama[2☯], Teiichiro Shiino[3], Takeyuki Suzuki[4], Yoshiaki Ishigatsubo[4], Atsuhisa Ueda[4], Akira Shirai[5], Mitsuhiro Takeno[4], Satoshi Hayakawa[6], Shigehiro Sato[7], Osamu Tochikubo[1], Shingo Kiyoura[8], Kaori Sawada[9], Takashi Ikegami[9], Tadahito Kanda[2], Katsuhiko Kitamura[1], Hironori Sato[2*]

1 Department of Public Health, Yokohama City University School of Medicine, Kanagawa, Japan, **2** Center for Pathogen Genomics, National Institute of Infectious Diseases, Tokyo, Japan, **3** AIDS Research Center, National Institute of Infectious Diseases, Tokyo, Japan, **4** Department of Internal Medicine and Clinical Immunology, Yokohama City University Graduate School of Medicine, Kanagawa, Japan, **5** College of Nursing, Yokohama City University School of Medicine, Kanagawa, Japan, **6** Department of Pathology and Microbiology, Nihon University School of Medicine, Tokyo, Japan, **7** Department of Bacteriology, Iwate Medical University, Iwate, Japan, **8** SGI Japan, Ltd, Tokyo, Japan, **9** Ryoka Systems Inc., Tokyo, Japan

Abstract

The third variable region (V3) of the human immunodeficiency virus type 1 (HIV-1) envelope gp120 subunit participates in determination of viral infection coreceptor tropism and host humoral immune responses. Positive charge of the V3 plays a key role in determining viral coreceptor tropism. Here, we examined by bioinformatics, experimental, and protein modelling approaches whether the net positive charge of V3 sequence regulates viral sensitivity to humoral immunity. We chose HIV-1 CRF01_AE strain as a model virus to address the question. Diversity analyses using CRF01_AE V3 sequences from 37 countries during 1984 and 2005 ($n = 1361$) revealed that reduction in the V3's net positive charge makes V3 less variable due to limited positive selection. Consistently, neutralization assay using CRF01_AE V3 recombinant viruses ($n = 30$) showed that the reduction in the V3's net positive charge rendered HIV-1 less sensitive to neutralization by the blood anti-V3 antibodies. The especially neutralization resistant V3 sequences were the particular subset of the CCR5-tropic V3 sequences with net positive charges of +2 to +4. Molecular dynamics simulation of the gp120 monomers showed that the V3's net positive charge regulates the V3 configuration. This and reported gp120 structural data predict a less-exposed V3 with a reduced net positive charge in the native gp120 trimer context. Taken together, these data suggest a key role of the V3's net positive charge in the immunological escape and coreceptor tropism evolution of HIV-1 CRF01_AE *in vivo*. The findings have molecular implications for the adaptive evolution and vaccine design of HIV-1.

Citation: Naganawa S, Yokoyama M, Shiino T, Suzuki T, Ishigatsubo Y, et al. (2008) Net Positive Charge of HIV-1 CRF01_AE V3 Sequence Regulates Viral Sensitivity to Humoral Immunity. PLoS ONE 3(9): e3206. doi:10.1371/journal.pone.0003206

Editor: Linqi Zhang, AIDS Research Center, Chinese Academy of Medical Sciences and Peking Union Medical College, China

Received June 17, 2008; **Accepted** August 21, 2008; **Published** September 12, 2008

Funding: This work was supported by grants from the Ministry of Health, Labor and Welfare for HIV/AIDS research, and the IMAI Memorial Trust for AIDS Research, Japan.

Competing Interests: The authors have declared that no competing interests exist.

* E-mail: hirosato@nih.go.jp

☯ These authors contributed equally to this work.

Introduction

The third variable region (V3) of human immunodeficiency virus type 1 (HIV-1) envelope gp120 subunit participates in determination of viral infection coreceptor tropism [1,2]. It is usually composed of 35 amino acids, which form a loop-like structure on the gp120 monomer [3,4]. The V3 and the conserved outer domain of gp120 create the binding surface for viral infection coreceptors after the binding of gp120 to the primary infection receptor CD4 [4,5]. These interactions and successive conformational changes of gp120 are essential in rendering the initially occluded hydrophobic domain of the envelope gp41 subunit available to fusion with cellular plasma membrane.

The HIV-1 V3 is highly variable. In parallel with the V3 sequence variation, many types of infection coreceptors are reported. These are the members of the G protein-coupled receptor superfamily. The two most common types of infection coreceptors in humans are the CC chemokine receptor 5 (CCR5) and the CXC chemokine receptor 4 (CXCR4) [6]. Notably, a single group of the HIV-1 variants using the CCR5 (R5 virus [6]) predominates during the first several to 10 years or more of persistent infection *in vivo* [7,8]. Other tropism variants including CXCR4-tropic variants (X4 virus [6]) can grow at early stage of infection by needle stick injuries, but are replaced with the R5 viruses after seroconversion [9,10]. They generally grow better only during progression to AIDS. The R5 and X4 viruses are distinguishable by sequence feature of V3: the R5 V3 amino acid sequences generally have a lower net positive charge than those of X4 [3,11]. Only a few basic substitutions in V3 can switch the viral coreceptor tropism from CCR5 to CXCR4 [12,13]. Considering the extremely high levels of mutation rate of HIV-1, these findings suggest that strong selective forces are continually purifying the R5 viruses during long-lasting persistent infection.

The HIV-1 V3 is highly immunogenic, tolerant to change, and variable presumably to evade immune recognition [14–16]. HIV-infected individuals make high levels of anti-V3 antibodies that are

reactive with soluble, monomeric gp120 protein [17,18]. However, they often react poorly or only with low affinity to the native, oligomeric form of the gp120 protein [17,18]. The inaccessibility of the oligomeric envelope protein is particularly prominent in the primary HIV-1 isolates [19–21], which are usually the R5 viruses. Indeed, studies with limited set of viruses have shown that antibodies reactive with the R5-virus V3s tend to bind to the monomeric but not the oligomeric gp120s [22,23], and they poorly neutralize the R5 viruses [23–25]. In contrast, antibodies against X4-virus V3s usually bind to both forms of gp120s [22,23], and they potently neutralize the X4 viruses [23–25]. Consistent with the lower sensitivity of R5 viruses to anti-V3 antibody neutralization, positive selection for amino acid variation is less prominent in the R5 virus V3 sequences, and V3 amino acid sequences of the R5 virus are relatively homogeneous among virus isolates [26,27] or in infected individuals [28–30] compared with those of the X4 viruses.

While the immunological escape, variation, and coreceptor tropism evolution of HIV-1 is an important issue from both clinical and scientific viewpoints, current studies are largely confined to those of HIV-1 subtype B from North America and Europe. In this study, we attempted to obtain and integrate information on HIV-1 CRF01_AE strain [31] circulating in Southeast Asia. Specifically, we examined whether net positive charge of HIV-1 CRF01_AE V3 sequence regulates viral sensitivity to humoral immunity. Here, we demonstrate by combining bioinformatics, experimental, and protein modelling approaches that the reduction in net positive charge of HIV-1 CRF01_AE V3 sequence reduces viral sensitivity to humoral immunity and simultaneously confers viral CCR5 tropism. The findings suggest a key role of the V3 net positive charge in the immunological escape, variation, and the coreceptor-tropism evolution of HIV-1 CRF01_AE *in vivo*.

Results

Correlation of HIV-1 CRF01_AE V3 net positive charge, V3 prevalence, and V3 diversity.

A previous case study has suggested that a group of CRF01_AE V3 sequences for the viral CCR5 tropism is resistant to the selective force for amino acid variation [29,30]. To extend this finding with three infected individuals, we conducted large-scale analysis of V3 diversity using public database information. V3 sequences of the CRF01_AE strain were extracted from the HIV Sequence Database (http://www.hiv.lanl.gov/content/hiv-db/mainpage.html). A single V3 amino acid sequence per infected individual was randomly extracted. Sequences with ambiguous bases are excluded from the analysis. V3 sequences ($n = 1361$, 35 amino acid length) from 37 countries during 1984 and 2005 (see supporting information Figs. S1a and S1b) were used for the diversity analysis. The 1361 V3 sequences were divided into two subsets, "a" and "b", which lack and have the glycosylation motif, respectively. Each group was divided into subgroups on the basis of the net charge; arginine, lysine, and histidine were counted as +1, aspartic acid and glutamic acid as −1, and other amino acids as 0.

Although there are exceptions, the V3 amino acid sequences capable of directing the viral CCR5 tropism of the CRF01_AE strain generally have net positive charges of +2 to +4 and the conserved N-linked glycosylation motif (asparagine-X-threonine/serine) at positions 6 to 8 [29,30]. Consistent with the dominance of the R5 viruses in humans, less positively charged, glycosylated V3 sequences for the CCR5 tropism (2b, 3b, and 4b) were dominant in the database for over 15 years, independent of the sampling period (Fig. 1A and Fig. S1c). Shannon entropy scores representing amino acid variation were relatively low for the most abundant 3b V3 compared to those for the 7a V3 for the CXCR4 tropism (Fig. 1B), consistent with previous report [3]. Nucleotide substitutions for amino acid change were more suppressed in the V3s for the CCR5 tropism compared with those for the CXCR4 tropism (Fig. 1C). The 3b V3 had the lowest ratio of nonsynonymous to synonymous substitutions (d_n/d_s) with about 0.6, and acquisition of a glycosylation site decreased the d_n/d_s ratios ($P = 0.001$, Table S1). The d_n/d_s ratios correlated positively with the Shannon entropies, with lower d_n/d_s ratios for lower entropies (Fig. 1D). Similar effects of the net positive charge of V3 on V3 diversity were detected in other major genetic lineages of HIV-1 circulating in the world, such as subtypes A, B, and C (Fig. S2).

If the low levels of amino acid changes in the V3 structures for CCR5 tropism involved the elimination of new mutants in natural selection, negative values for Tajima's D statistic would be expected [32]. Indeed, Tajima's D statistic was significantly negative for 2b and 3b V3s ($P = 0.01$, Fig. 1E and Table S2). Together, these findings on V3 diversity provide further evidence that the V3 sequences for the CCR5-tropism are less variable in nature due to the limited positive selection for amino acid diversity compared with those for CXCR4 tropism.

Correlation of HIV-1 CRF01_AE V3 net positive charge, HIV-1 neutralization sensitivity, and HIV-1 coreceptor tropism.

A positive selection pressure for the V3 diversity can be the humoral immunity. To examine whether the V3 net positive charge regulates HIV-1 neutralization sensitivities to the anti-V3 antibodies, we used V3 recombinant viruses ($n = 30$). The recombinant viruses have the CRF01_AE V3s in the backbone of the X4 virus gp120 of HIV-1 subtype B, LAI strain [13,30,33]. The V3s were from HIV-1 proviral DNA clones in the peripheral blood mononuclear cells of three infected individuals at the asymptomatic stage or AIDS [13,30,33]. These V3s could be grouped into the 2b ($n = 2$), 3b ($n = 4$), 4b ($n = 5$), 5b ($n = 3$), 6b ($n = 5$), 3a ($n = 1$), 4a ($n = 2$), 5a ($n = 3$), 6a ($n = 3$), and 7a ($n = 2$) sequences (Fig. S3). The 2b, 3b, and 4b V3 clones were the most prevalent in the three infected individuals examined, and their sequences were mostly identical [29], consistent with the V3 prevalence and diversity data in this study. The neutralization sensitivity of each recombinant virus was assessed with a single-round viral infectivity assay [34]. In parallel, titers of plasma antibody reactive with the V3 elements of the recombinant viruses were measured with V3-peptide-based, enzyme-linked immunosorbent assay (ELISA) [35].

When the V3 synthetic peptide of the parental virus of the recombinant viruses was used for the immunoassay, the CRF01_AE plasma samples had only traces of binding antibodies (Fig. 2B, Absorbance of LAI). The blood samples failed to neutralize this virus (Fig. 2B, ND_{50} of LAI). Thus, the blood samples tested are lacking in anti-V3 binding antibodies, as well as neutralization antibodies against the parental subtype B virus. The results agree with low levels of V3 amino acid identities between subtype B and CRF01_AE strains (http://www.hiv.lanl.gov/content/hiv-db/mainpage.html). They also agree with the assumption that V3 sequence diversity causes neutralization escape of HIV-1.

All blood samples from CRF01_AE infected individuals contained antibodies that bound to the synthetic peptides from the CRF01_AE strain V3 sequences of the recombinant viruses (Fig. 2B, Absorbance of 2b to 7a). Coincidentally, they neutralized a group of the viruses having particular V3 sequences (Fig. 2B). The neutralization-sensitive viruses had V3s lacking a glycosylation site (3a, 4a, 5a, 6a, 7a, $n = 11$), or V3s having a glycosylation

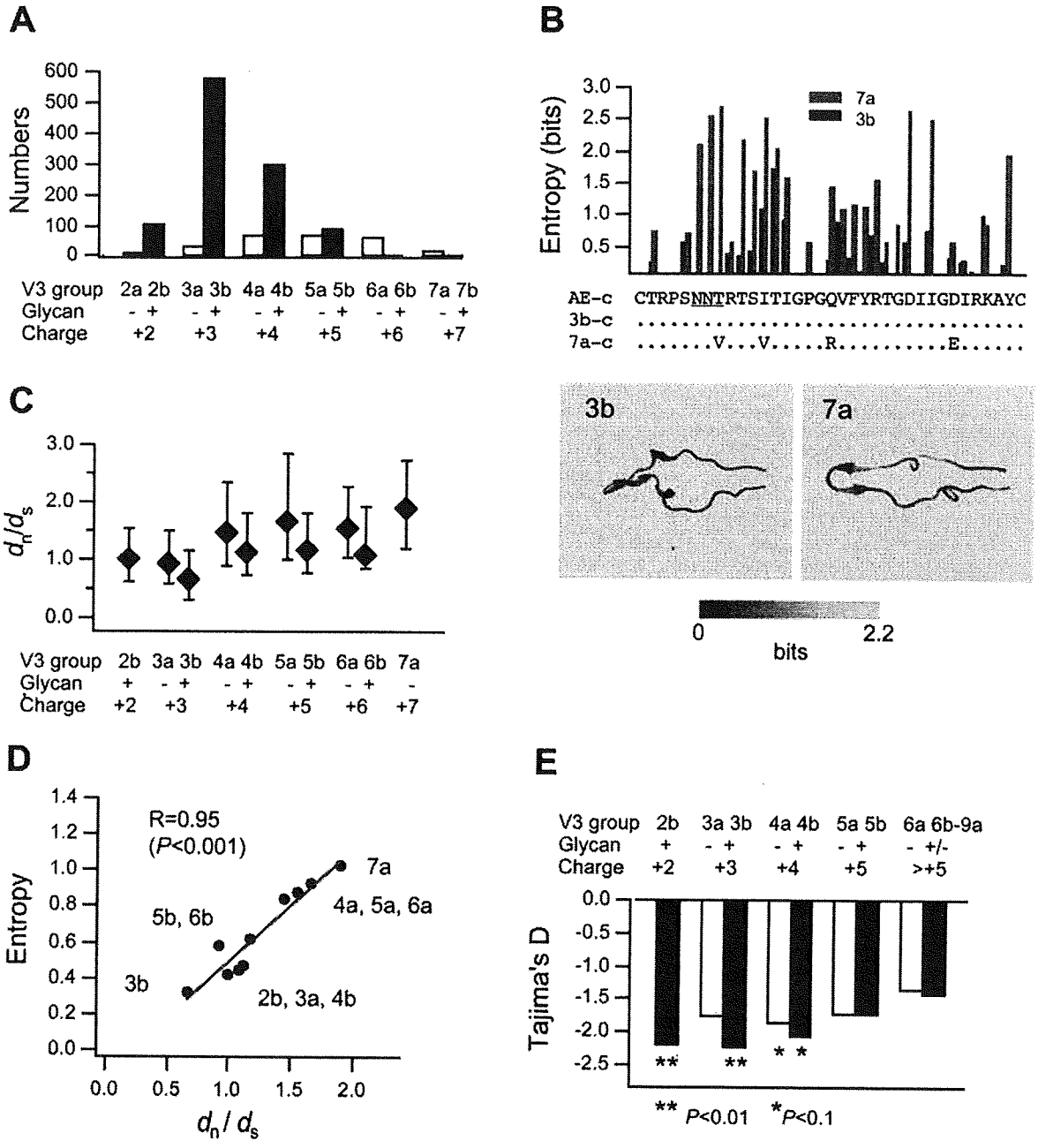

Figure 1. V3 net positive charge influences V3 diversity. HIV-1 CRF01_AE V3 sequences ($n = 1361$) were grouped on the basis of net positive charge and glycosylation capability *(A)* Distribution of the V3 structural variants of HIV-1 CRF01_AE in the public database. *(B)* Shannon entropy scores [3] on primary and three-dimensional structures of 3b and 7a V3s. AE-c, 3b-c, and 7a-c indicate consensus sequences for all CRF01_AE sequences, 3b V3 group ($n = 576$), and 7a V3 group ($n = 21$), respectively. *(C)* Median (diamond) and interquartile range (vertical bar) of ratios of d_n/d_s, *(D)* Relation of median d_n/d_s ratios and average Shannon entropy scores, and *(E)* Tajima's D statistic values [32] for each V3 structural group.
doi:10.1371/journal.pone.0003206.g001

site and increased net positive charge (5b and 6b, $n = 8$) (Fig. S3). The neutralization activities were abrogated by protein G pre-treatment of the plasma samples (Fig. S4), showing that neutralization is indeed mediated by antibodies in the plasma samples.

Notably, the blood samples poorly neutralized a group of V3 recombinant viruses (Fig. 2B, ND_{50} of 2b, 3b, and 4b, $n = 11$). These viruses had weakly charged V3s and had an N-glycosylation site, which are the characteristics of V3s for CCR5 tropism (Fig. S3, V3 IDs of 2b, 3b, and 4b). The lack of neutralization activities was not

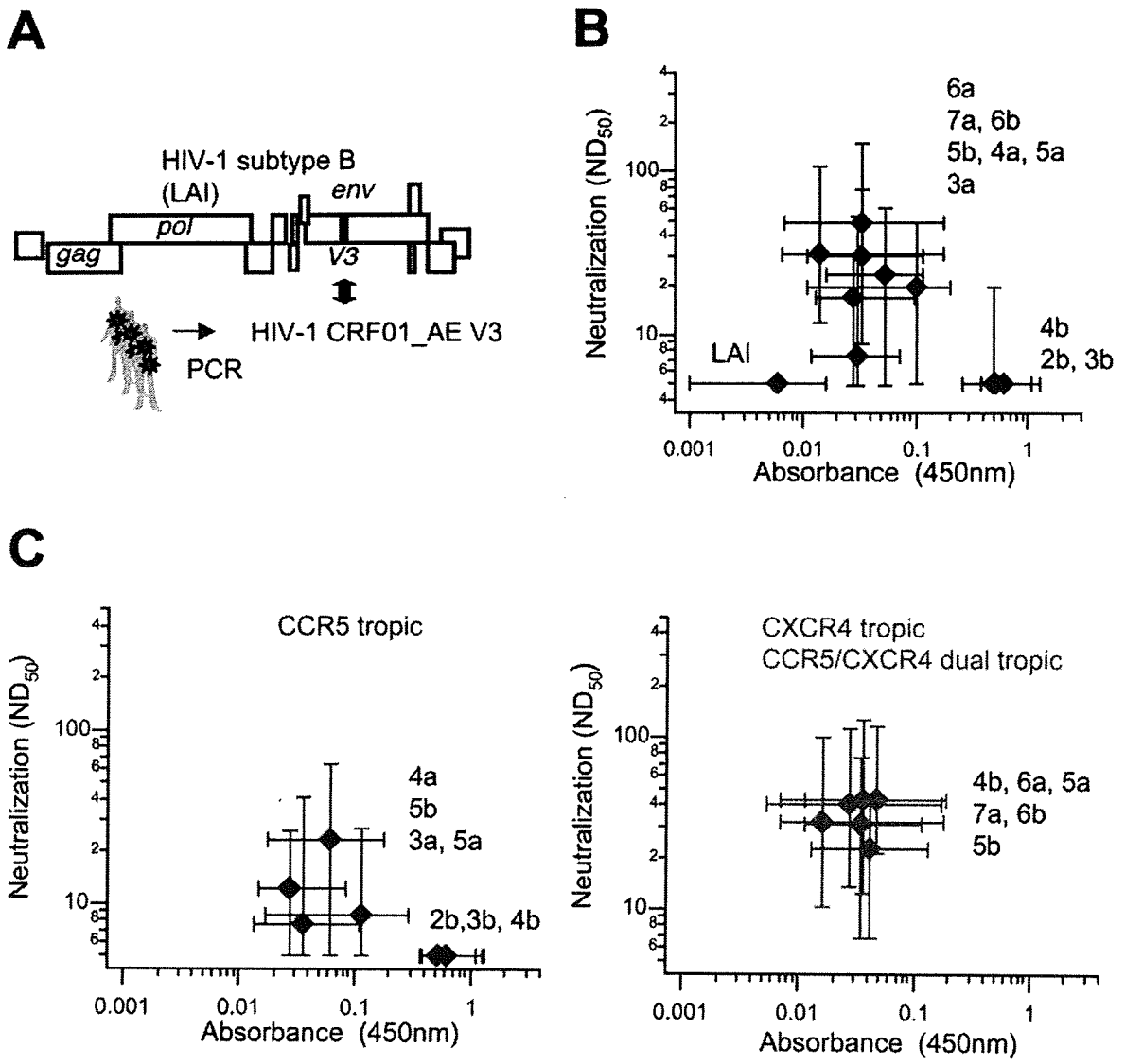

Figure 2. Reduction in V3 net positive charge causes loss of HIV-1 neutralization sensitivity to blood antibodies against V3 PND. *(A)* Genome structure of the V3 recombinant viruses ($n = 30$) [13,30,33]. *(B)* Blood anti-V3 antibody titers and viral neutralization sensitivity to the blood antibodies. Plasma samples ($n = 20$) were obtained from CRF01_AE positive individuals. Plasma antibody binding activities to the synthetic peptides corresponding to each V3 PND of the recombinant viruses were measured by V3-peptide-based ELISA [35] (Absorbance at 450 nm). The same plasma samples were used to measure ND_{50} against recombinant viruses in a single-round infectivity assay using $CD4^+CXCR4^+CCR5^+$ HeLa cells [34] (Neutralization). Medians (diamond) and interquartile ranges for individual V3 structural groups are shown. *(C)* Neutralization sensitivity and coreceptor tropism. The recombinant viruses were grouped into CCR5-tropic (left) and CXCR4-tropic (right) variants using data reported previously [13,30,33].

doi:10.1371/journal.pone.0003206.g002

due to the lack of anti-V3 binding antibodies against these recombinant viruses. The blood samples contained high levels of antibodies that bound to the 2b, 3b, and 4b V3 peptides, more so than of other V3 groups (Fig. S5 and Fig. 2B, Absorbance of 2b, 3b, and 4b). The results are consistent with the high levels of prevalence and limited diversity of these V3 sequences (Fig. 1). The study shows that the group of V3 elements for CCR5 tropism is highly immunogenic, whereas binding antibodies raised in humans generally show only weak neutralization activities. This neutralization-resistant phenotype associated with particular V3 group was observed reproducibly in a multiple-round infectivity assay, suggesting that the phenotype is intrinsic to the viruses (Fig. S6).

The relation of this neutralization-resistant phenotype and HIV-1 coreceptor tropism was examined using information on coreceptor usages of the V3 recombinant viruses [13,30,33]. Importantly, the V3s having the viral-resistant phenotype unexceptionally rendered HIV-1 CCR5-tropic (Fig. 2C, left panel, V3 groups of 2b, 3b, and 4b, $n = 10$). On the other hand, V3s conferring CCR5 tropism did not always render HIV-1 resistant (Fig. 2C, V3 groups of 3a, 4a, 5a, and 5b, $n = 7$). Thus, the V3s

associated with the neutralization resistance are a subset of the V3 elements associated with viral CCR5 tropism. In contrast, all V3s associated with viral CXCR4 tropism and CCR5/CXCR4 dual tropism rendered HIV-1 susceptible to neutralization (Fig. 2C, V3 groups of 4b, 5a, 5b, 6a, 6b, and 7a, $n = 13$).

The group of viruses having 4b V3s were neutralization-resistant only when they had the CCR5-restricted tropism (Fig. 2C, 4b in left and right panels). The 4b V3s associated with viral neutralization resistance had no basic substitutions compared with the CRF01_AE consensus (Fig. S3, recombinant IDs of A1, A2, A4, and A5). By contrast, the neutralization-sensitive version had two basic substitutions (Fig. S3, recombinant ID of B10). The results may imply that V3 basic substitutions at particular positions in addition to the overall net positive charge play a critical role in the determination of viral neutralization sensitivity and coreceptor tropism.

We further examined whether a CCR5-tropic but not a CXCR4-tropic envelope of CRF01_AE strain is linked to viral resistant to neutralization by anti-V3 antibodies. For this purpose, we used a pair of nearly isogenic R5 and X4 virus clones that have 3b and 5a V3, respectively [36,37]. The results obtained with these clones and 35 blood specimens were consistent with present study and indicated that the CCR5-tropic but not the CXCR4-tropic envelope protein of the HIV-1 CRF01_AE strain was linked to viral resistance to neutralization with anti-V3 antibodies in the blood (data not shown).

HIV-1 V3 net positive charge and V3 conformation

To obtain molecular insights into the roles of the V3 net positive charge in regulating HIV-1 neutralization sensitivity, we conducted computer-aided structural analysis. Currently, X-ray structure information on the HIV-1 R5 virus gp120 monomer bound with soluble CD4 [3] is available in the Protein Data Bank. With the data, we attempted to obtain a gp120 monomer structure for the pre-CD4 binding stage to address initial V3 conformation before receptor interaction. We first constructed gp120 outer domain models of the V3 recombinant viruses used in this study by a homology modelling method. Molecular dynamics (MD) simulation was then performed with the homology models.

Figure 3A shows examples of the MD simulation of two recombinant virus gp120s with 3b and 7a V3 elements. The TH09 V3 (3b V3) is from an HIV-1 CRF01_AE infected asymptomatic patient, identical to the CRF01_AE V3 consensus sequence (Fig. S3, recombinant ID of TH09), rendered HIV-1 neutralization-resistant and CCR5-tropic (Fig. 2C, left panel). The B1 V3 (7a V3) is from an AIDS patient, more positively charged (Fig. S3, recombinant ID of B1) and rendered HIV-1 neutralization-sensitive and CXCR4-tropic (Fig. 2C, right panel).

The MD simulations show that V3 configuration is nearly equilibrated up to 5 nanoseconds of simulation times (Fig. 3A). Notably, the TH09 V3 was equilibrated at a much more distant position from the β20β21 loop in the outer domain than the B1 V3 (Figs. 3A and B). Hydrogen bonds were formed around the TH09 V3 base between D330 and R332, and D330 and R424, which contributed to stabilizing the V3 configuration (Fig. 3C). However, the hydrogen bonds were not formed with the gp120 having the B1 V3 (Fig. S7). Coulombic repulsion between B1 V3 and R424 increased about 44-fold as compared with that of TH09 V3, with electrostatic energies of +2.0 and +0.045 kcal/mole for B1 and TH09, respectively. The repulsion was greatest on the R424 residue in the gp120 outer domain. The results suggest that an increase in the V3 net positive charge influences electrostatic balance at the V3 base.

Importantly, the amino acids around the V3 base are relatively conserved in nature. The D330 and R332 are located at the V3 base and highly conserved within each subtype of the HIV-1 M group in the public database (Fig. 3D). The conservation was seen even in the V3s for the CXCR4 tropism (Fig. 1B). The R424 is in the fourth constant region (C4) of the gp120 core, and neighbouring amino acids are also conserved. The CRF01_AE strain alone has lysine at position 424, whereas K424 is conserved within the CRF01_AE. These data suggest that most HIV-1 gp120 monomers have the potential to stabilize V3 configuration at the base and that basic amino acid substitutions in V3 have strong influences on the V3 configuration.

The MD simulation data were incorporated into those of a gp120 trimer structure obtained by cryoelectron microscopy [38] to illustrate schematically the V3 position in the native gp120 trimer (Fig. 4). Some glycans are also schematically illustrated at the appropriate regions. The models predict that less positively charged V3 protrudes into the outer domain of the neighboring gp120 monomer, whereas V3 with increased net positive charge protrudes away from the neighboring monomer in the trimer context.

Discussion

HIV-1 is the causative agent of AIDS and is responsible for more than 2 million deaths every year. Understanding the immunological escape, variation, and coreceptor tropism evolution of HIV-1 is critical for developing strategies for anti-HIV interventions. In this regard, current studies are largely confined to those of HIV-1 subtype B from North America and Europe. In this study, we focused on the study of HIV-1 CRF01_AE strain circulating in Southeast Asia. The HIV-1 CRF01_AE is one of the five major HIV-1 subtypes circulating in the world [31] and thus an important strain for public health of Asia, as well as of world. However, much less basic information are available as compared with the HIV-1 subtype B.

We first demonstrate with bioinformatics approach using 1361 sequences in public database that CRF01_AE V3's net positive charge influences V3 diversity and prevalence. We found that the net positive charge of V3 influences V3 diversity (Fig. 1). Acquisition of the N-glycosylation motif in V3 augmented the sequence conservation. Our data of d_n/d_s ratios and Tajima's D statistic provide strong evidence that the reduction in V3 diversity is due to limited positive selection for amino acid changes. These findings are compatible with previous findings with subtype B that sequence diversity is smaller among R5 virus V3s [26–28]. Moreover, the findings demonstrate the generality of findings obtained with an intra-familial infection case of CRF01_AE infection [29,30]. The evidence that the V3 net positive charge influences V3 diversity is not solely based on sequence analysis. Structural and neutralization data suggest that V3 net positive charge regulates V3 diversity by controlling V3 structure and neutralization sensitivities, as discussed below.

We next examined potential causes of the differential diversity of CRF01_AE V3 sequences. We demonstrated with neutralization assay of V3 recombinant viruses that the V3 net positive charge influences HIV-1 neutralization sensitivity. We found that reduction in the net positive charge of V3 caused reduction in viral neutralization sensitivity to the blood anti-V3 antibodies in infected humans (Fig. 2). Again, acquisition of the N-glycosylation motif in V3 augmented the effect. We further confirmed that the especially neutralization resistant V3 sequences all render HIV-1 CCR5 tropic (Fig. 2C). These results are compatible with previous findings with subtype B that R5 viruses are more refractory to anti-

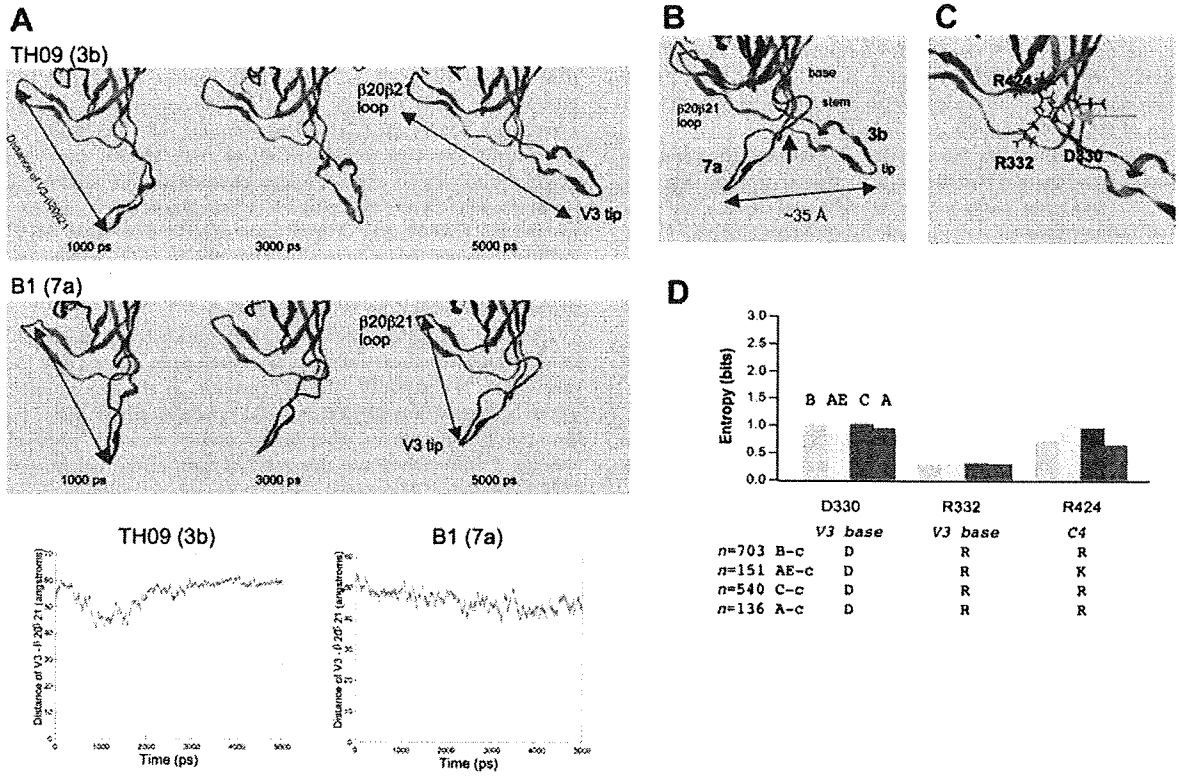

Figure 3. MD simulation of the HIV-1 gp120 outer domain. The V3 subset conferring the neutralization-resistant phenotype is referred to in this study as rV3: it has net positive charges of +2 to +4, an N-glycosylation site, and a capability to direct viral CCR5 tropism. The non-rV3 renders HIV-1 more susceptible to blood antibody neutralization. It has net positive charges of greater than +4 and a capability to direct viral CXCR4 tropism. *(A)* Examples of the MD simulation of two recombinant virus p120 outer domains with rV3 (TH09) and non-rV3 (B1). Distance between the Cα atom of P318 at the V3 tip and the Cα atom of Q433 at the β20β21 loop were monitored for 5 nanoseconds. *(B)* Superimposition of the gp120 monomers with the TH09 V3 (blue) or B1 V3 (red) at the simulation time of 5 nanoseconds. *(C)* Close-up view of the base-stem region of the TH09 V3. Orange dotted lines around the tip of the orange arrow indicate three hydrogen bonds at the V3 base. *(D)* Shannon entropy scores of the amino acids at the positions of 330, 332, and 424 in the public database. The positions in the gp120 of the HIV-1_{LAI} [48] are used for the amino acid numbering.
doi:10.1371/journal.pone.0003206.g003

V3 antibodies [23–25]. Together with sequence analysis data, these findings suggest that anti-V3 antibodies can act as a positive selection pressure to increase V3 sequence diversity and that V3 positive net charge can influence V3 diversity by regulating neutralization sensitivity to the V3 antibodies.

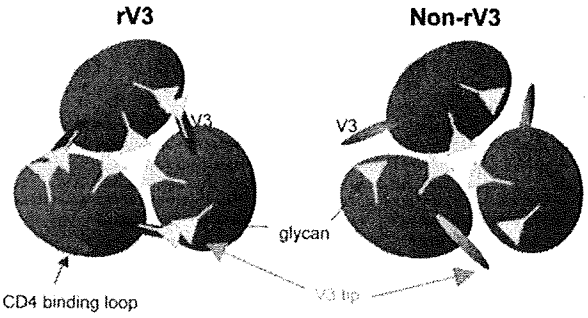

Figure 4. Models for the self-directed masking of V3 by mutations for the CCR5 tropism. The MD data in Fig. 3 and the HIV-1 gp120 trimer structure from cryoelectron microscopy [38] were used to construct the gp120 trimer models with CCR5-tropic (left) or CXCR4-tropic (right) V3. The models were made so that the MD data and experimental data [3,4,38] are compatible.
doi:10.1371/journal.pone.0003206.g004

Importantly, present data revealed that not all the CCR5-tropic V3 sequences render HIV-1 resistant to the neutralization. Some V3 sequences lacking N-glycosylation site or those have the glycosylation site but have net positive charge of +5 conferred CCR5 tropism on HIV-1, whereas they were relatively sensitive to the antibody neutralization (Fig. 2C). These data are consistent with findings on CRF01_AE V3 sequence diversity and prevalence in this study. Together, the data suggest that a particular subset of CRF01_AE V3 for CCR5 tropism confers a selective advantage on HIV-1 in the face of humoral immunity and that the anti-V3 antibodies may be an important selective force to maintain CCR5-tropic V3 sequences with limited amino acid changes during persistent infection.

We further examined molecular mechanisms of neutralization escape. We found with MD simulation that reductions in the net positive charge of V3 caused a shift of V3 position in the gp120 monomer (Fig. 3). This is the first indication that the net positive charge of V3 regulates V3 configuration in the gp120 monomer. By incorporating our MD data into experimental data of HIV-1 gp120 structures [3,4,38], we proposed a model of V3 masking that explains how the net positive charge of V3 regulates HIV-1 V3 neutralization sensitivity (Fig. 4). The model explains present

diversity and neutralization data: it predicts that less positively charged V3 for CCR5 tropism positions in the gp120 trimer context such that it protrudes into the outer domain of the neighboring gp120 monomer, which will inevitably result in better protection of V3 from antibodies by the glycans. This model also explains why anti-V3 antibodies bind effectively to monomeric but not native, oligomeric form of the gp120 protein of the HIV-1 R5 viruses [22–25]. Further structural studies are under way to assess the model.

Our study provides molecular insights into the mechanisms of coreceptor-tropism evolution of HIV-1. Due to high levels of viral mutation rate, vigorous and continual viral replication *in vivo*, and viral tolerance to V3 mutations, many viable HIV-1 V3 mutants would be continuously generated during a persistent infection. Therefore, why only the R5 virus dominates during persistent infection is a long-lasting question in HIV-1 research. Our study suggests a selective advantage of a subset of CCR5-topic V3 sequences in the face of humoral immunity: self-masking of neutralization epitope by reduction in net positive charge. Higher levels of the d_n/d_s ratios for more positively charged V3 sequences for CXCR4 tropism (Figs. 1C and D) may imply that the X4 viruses might persist as a minority, continually receive positive selection pressures for amino acid changes, and outgrow only when the host immunity is severely damaged.

It will be important to examine why neutralization resistant V3 sequences exclusively direct viral CCR5 usage (Fig. 2C). The distinct V3 configuration in gp120 may contribute to the restriction of coreceptor type to be interacted, because amino acid residues at the V3 base directly participate in the binding to the N-terminal region of CCR5 [4]. In addition, structural differences among chemokine receptors may contribute. For example, the N-terminal region of CXCR4 is glycosylated, whereas that of CCR5 is not. The .glycosylated V3 for neutralization resistance will sterically interrupt the access to the glycosylated coreceptor. Indeed, the removal of the N-linked glycosylation sites from CXCR4 allows the protein to serve as a universal coreceptor for both X4 and R5 viruses [39]. Further structural studies are under way to address this issue.

Our study has implications for HIV-1 vaccine design. The data suggests that a key impediment to the clinical use of Gp120 as an immunogen may be the cryptic nature of the R5 virus V3 neutralization epitope. A simple strategy to use R5 virus Gp120 will be insufficient even if the Gp120 of circulating HIV-1 subtype is carefully selected as immunogen. To develop strategies that could circumvent or overcome the impediment may be critical for practical application of Gp120 vaccine. In this regard, the amino acids that contribute to forming V3 conformation for the epitope masking through hydrogen bonds are relatively conserved among HIV-1 major subtypes in the world (Fig. 3D). Therefore, intervention in these interactions might be a target for a new strategy to improve effectiveness of immunological control of HIV-1.

In conclusion, we have identified here structural and functional features of HIV-1 CRF01_AE V3 elements those allow HIV-1 less sensitive to antibody neutralization. To our knowledge, this is the first report to show that the net positive charge of a neutralization epitope regulates viral sensitivity to humoral immunity. Thus, amino acid substitutions altering charged status of antigen site appear to deserve more attention, particularly in the adaptive evolution of HIV-1, as well as the other rapidly evolving pathogen.

Materials and Methods

Analysis of sequence diversity

Grouping of the sequences was done computationally using a software system, InforSense BioSense V3 (InforSense Ltd. http://www.inforsense.com). Nonsynonymous and synonymous nucleotide substitutions were calculated for all pair-wise sequence comparisons within each V3 subgroup using the Perl version of SNAP (Los Alamos HIV sequence database) according to the Nei and Gojobori method [40] incorporating the statistical method developed by Ota and Nei [41]. Amino acid variation at individual V3 positions was calculated according to the method described in the report by Huang et al [3] on the basis of Shannon's equation [42]:

$$H(i) = -\sum_{x_i} p(x_i)\log_2 p(x_i)\ (x_i = \mathrm{G, A, I, V, ...}),$$

where $H(i)$, $p(x_i)$, and i indicate the amino acid entropy score of a given position, the probability of occurrence of a given amino acid at the position, and the number of the position, respectively. An $H(i)$ score of zero indicates absolute conservation, whereas 4.4 indicates complete randomness. The $H(i)$ scores were expressed in the V3 sequence or in the three-dimensional structures constructed by the MD simulation method described below. The $p(x_i)$ scores were used to construct a consensus for each V3 structural group. Tajima's D statistic [32] for each type of V3 sequence population was calculated using DnaSP 4.10 [43].

Blood specimens

Plasma samples were obtained from HIV-1 CRF01_AE positive individuals with written informed consent at Yokohama City University Hospital in Japan according to the rule of the ethics committee of the hospital. The clinical stages of the patients at the time of blood collection were A1 ($n=4$), A2 ($n=4$), B3 ($n=3$), C2 ($n=1$), C3 ($n=7$), and unknown ($n=1$) according to the 1993 Revised Classification System (CDC, USA). The $CD4^+$ T-cell counts and HIV-1 RNA levels ranged from 2×10^3 to 3719×10^3 / ml blood (mean = 243×10^3 /ml) and from <50 to 7.5×10^5 copies/ ml blood (mean = 2.4×10^4 copies/ml), respectively. All plasma samples were heat-inactivated at 56°C for 30 minutes prior to use.

Anti-V3 antibody titration

V3-peptide-based ELISA [35] was carried out using synthetic peptides matching to the central 19 amino acids of the V3 regions of the recombinant viruses (Fig. S3). Synthetic peptides were coated on 96-well plates (Immulon II; Dynatech Laboratories, Virginia, USA) and reacted with diluted plasma samples ($1/10^4$). Antibodies bound to the peptides were detected with anti-human IgG peroxidase conjugate and 3,3′,5,5′-tetramethylbenzidine substrate (TMB peroxidase EIA substrate Kit, Bio-Rad Laboratories, USA). Each plasma sample was tested in duplicate.

Neutralization assays

Plasmid DNAs containing HIV-1 V3 recombinant proviruses ($n=30$) were constructed by the overlap extension method [13,30,33]. Cell-free viruses were prepared by transfection of the plasmid DNAs into HeLa cells as described previously [13,30,33]. Neutralization activities were measured in a single-round viral infectivity assay using $CD4^+CXCR4^+CCR5^+$ HeLa cells [34]. Equal infectious titers of viruses (300 blue-cell-forming units) were incubated with serially diluted plasma samples ($1/10$ to $1/10^3$) for 60 min at 37°C. The infected cells were cultured for 48 hours at 37°C, fixed, and stained with 5-bromo-4-chloro-3-indolyl-β-D-galactopyranoside. Each plasma dilution was tested in duplicate, and the means of the positive blue cell numbers were used to calculate the 50% inhibition dose of viral infectivity (ND_{50}). For plasma samples that did not neutralize a virus at the lowest dilution tested (1:10), an arbitrary titer of 1:5 (50 ND_{50} /ml) was

used. In some cases, neutralization activities were measured using a multiple-round viral infectivity assay using NP-2 cell lines [44]. Equal infectious titers of the viruses (100 tissue culture infectious dose) were incubated with serially diluted plasma samples (1/10 to $1/10^3$) for 60 min at 37°C and used to infect the $CD4^+CXCR4^+$ NP-2 cells and $CD4^+CCR5^+$ NP-2 cells. After 60 min, the cells were washed once with phosphate-buffered saline. Culture supernatants were collected at 5 days after infection, and amounts of HIV-1 Gag p24 proteins were measured with a commercially available kit (RETROtek HIV-1 p24 Antigen ELISA, ZeptoMetrix Corporation, USA). Each plasma dilution was tested in duplicate, and the means of the p24 amounts were used to calculate the ND_{50}.

HIV-1 coreceptor usages

Previous data of the coreceptor tropisms of the recombinant viruses [13,30,33] were used.

MD simulation

Gp120 outer domain structures bearing various V3 elements were constructed with the homology modelling technique, using the Molecular Operating Environment, MOE 2006.08 (Chemical Computing Group Inc., Montreal, Quebec, Canada) as described [45,46]. As the modelling template, we used the crystal structure of HIV-1 gp120 containing an entire V3 element at a resolution of 3.30Å (PDB code: 2B4C), which represents the structure after the CD4 binding [3]. The 251amino-terminal and 24 carboxyl-terminal residues were deleted to construct the gp120 outer domain structure. MD simulations were performed using the SANDER module in the AMBER 8 program package [47] with MDGRAPE-3 (http://mdgrape.gsc.riken.jp/) and the AMBER parm99 force field with the TIP3P water model. After heating calculations for 20 picoseconds until 310 K using the NVT ensemble, the simulations were executed using the NPT ensemble at 1 atm and at 310 K for 5 nanoseconds. Superimpositions of the structures were done by coordinating atoms of amino acids along the β-sheet at the V3 base.

Supporting Information

Figure S1 Information on the V3 sequences for the diversity analyses. Shown are the % distributions of CRF01_AE V3 sequences used in the present study ($n = 1361$) as a function of sampling years (a), countries (b), and V3 structural group (c). The sequences during 1991 to 2005 ($n = 1148$) represent a majority. They are mostly from Asia (15 countries, 1219 sequences). Others are from Africa (7 countries, 52 sequences), Europe (10 countries, 47 sequences), other regions (5 countries, 36 sequences), and unknown (1 sequence). V3 groups having CCR5 tropism (2b, 3b and 4b) represent the majority independent of the sampling period.
Found at: doi:10.1371/journal.pone.0003206.s001 (0.34 MB TIF)

Figure S2 V3 diversity of HIV-1 subtypes A, B, and C. Global distribution (left) and $_{dn}/_{ds}$ ratios (right) of V3 structural variants of HIV-1 subtypes A, B, and C were examined, using the HIV-1 public database information from June 2007, and plotted as described in Fig. 1C.
Found at: doi:10.1371/journal.pone.0003206.s002 (0.31 MB TIF)

Figure S3 V3 amino acid sequences of the recombinant viruses. V3 sequences of the recombinant viruses are from CRF01_AE clones in uncultured peripheral blood mononuclear cells from a Japanese family [30] (V3 IDs of A1{similar, tilde operator }A9 and B1{similar, tilde operator }B13), A1 variants having naturally occurring basic amino acid substitutions (mt1{similar, tilde operator }mt8) [13], and TH09 isolate having the CRF01_AE consensus V3 sequence [33] (TH09). Deduced amino acids of the V3 sequences were aligned with the CRF01_AE consensus sequence, ENSI-c. The small blue open box indicates a potential N-linked glycosylation site conserved in the V3 structural group b. Red letters indicates basic amino acid substitutions with respect to ENSI-c. The large black box indicates 19 amino acid sequences used for V3-peptide ELISA in Fig. 2. The net charge is the number of positively charged amino acids (R, K, and H) minus the number of negatively charged amino acids (D and E). Coreceptor tropism of the recombinant viruses was determined using $CD4^+CXCR4^+$ HOS cells and $CD4^+CCR5^+$ HOS cells [13,30,33].
Found at: doi:10.1371/journal.pone.0003206.s003 (0.39 MB TIF)

Figure S4 Effects of protein G on plasma neutralizing activities. The plasma samples (YM17 and YM61) were incubated with serially diluted protein G agarose solution (GammaBind Plus Sepharose, Amersham) for 60 min at 37°C. The agarose was removed by brief centrifugation, and the supernatants were used to measure ND_{50} against LAI recombinant viruses having non-rV3 (B1 and B10) using $CD4^+CXCR4^+CCR5^+$ HeLa cells (MAGIC-5 cells [34]) as described in Materials and Methods.
Found at: doi:10.1371/journal.pone.0003206.s004 (0.21 MB TIF)

Figure S5 Antibody epitope mapping of the rV3. Peptide-based, enzyme-linked immunosorbent assay [35] was carried out using indicated synthetic peptides matching the rV3 amino acids of the recombinant viruses (SI Fig. 3, recombinant ID of A1). Antibodies bound to the peptides were detected with anti-human IgG peroxidase conjugate and 3,3′,5,5′-tetramethylbenzidine substrate. Absorbance at 450 nm is shown.
Found at: doi:10.1371/journal.pone.0003206.s005 (0.27 MB TIF)

Figure S6 ND_{50} in the single- and multiple-round viral infectivity assays. Plasma samples ($n = 8$) were used to measure ND_{50} against LAI recombinant viruses having rV3 (clone IDs of ENSI-c and A1) and non-rV3 (B6). The ND_{50} were measured in a single-round viral infectivity assay using $CD4^+CXCR4^+CCR5^+$ HeLa cells (MAGIC-5 cells) [34] or a multiple-round viral infectivity assay using $CD4^+CXCR4^+$ NP2 cells and $CD4^+CCR5^+$ NP2 cells (NP-2 cells) [44] as described in Materials and Methods. Red diamonds indicate the medians of the neutralization titers of the 8 plasma samples.
Found at: doi:10.1371/journal.pone.0003206.s006 (0.20 MB TIF)

Figure S7 Close-up view of the V3 base-stem region of Gp120 with non-rV3. LAI Gp120 outer domain structures with B1 V3 were constructed computationally by methods of homology modelling and molecular dynamic simulation at a simulation time of 5 nanoseconds.
Found at: doi:10.1371/journal.pone.0003206.s007 (0.64 MB TIF)

Table S1
Found at: doi:10.1371/journal.pone.0003206.s008 (0.04 MB PDF)

Table S2
Found at: doi:10.1371/journal.pone.0003206.s009 (0.04 MB PDF)

Acknowledgments

We thank N. Yamamoto, T. Matano, and Y. Nagai for their helpful comments on the manuscript.

Author Contributions

Conceived and designed the experiments: SN MY HS. Performed the experiments: SN MY TS KK HS. Analyzed the data: SN MY TS HS. Contributed reagents/materials/analysis tools: SN MY TS YI AU AS MT SH SS OT SK KS TI TK KK HS. Wrote the paper: SN MY HS.

References

1. Hwang SS, Boyle TJ, Lyerly HK, Cullen BR (1991) Identification of the envelope V3 loop as the primary determinant of cell tropism in HIV-1. Science 253: 71–74.
2. Choe H, Farzan M, Sun Y, Sullivan N, Rollins B, et al. (1996) The beta-chemokine receptors CCR3 and CCR5 facilitate infection by primary HIV-1 isolates. Cell 85: 1135–1148.
3. Huang CC, Tang M, Zhang MY, Majeed S, Montabana E, et al. (2005) Structure of a V3-containing HIV-1 gp120 core. Science 310: 1025–1028.
4. Huang CC, Lam SN, Acharya P, Tang M, Xiang SH, et al. (2007) Structures of the CCR5 N terminus and of a tyrosine-sulfated antibody with HIV-1 gp120 and CD4. Science 317: 1930–1934.
5. Rizzuto CD, Wyatt R, Hernandez-Ramos N, Sun Y, Kwong PD, et al. (1998) A conserved HIV gp120 glycoprotein structure involved in chemokine receptor binding. Science 280: 1949–1953.
6. Berger EA, Doms RW, Fenyo EM, Korber BT, Littman DR, et al. (1998) A new classification for HIV-1. Nature 391: 240.
7. Scarlatti G, Tresoldi E, Bjorndal A, Fredriksson R, Colognesi C, et al. (1997) In vivo evolution of HIV-1 co-receptor usage and sensitivity to chemokine-mediated suppression. Nat Med 3: 1259–1265.
8. Connor RI, Sheridan KE, Ceradini D, Choe S, Landau NR (1997) Change in coreceptor use correlates with disease progression in HIV-1–infected individuals. J Exp Med 185: 621–628.
9. Cornelissen M, Mulder-Kampinga G, Veenstra J, Zorgdrager F, Kuiken C, et al. (1995) Syncytium-inducing (SI) phenotype suppression at seroconversion after intramuscular inoculation of a non-syncytium-inducing/SI phenotypically mixed human immunodeficiency virus population. J Virol 69: 1810–1818.
10. Pratt RD, Shapiro JF, McKinney N, Kwok S, Spector SA (1995) Virologic characterization of primary human immunodeficiency virus type 1 infection in a health care worker following needlestick injury. J Infect Dis 172: 851–854.
11. Cardozo T, Kimura T, Philpott S, Weiser B, Burger H, et al. (2007) Structural basis for coreceptor selectivity by the HIV type 1 V3 loop. AIDS Res Hum Retroviruses 23: 415–426.
12. Speck RF, Wehrly K, Platt EJ, Atchison RE, Charo IF, et al. (1997) Selective employment of chemokine receptors as human immunodeficiency virus type 1 coreceptors determined by individual amino acids within the envelope V3 loop. J Virol 71: 7136–7139.
13. Kato K, Sato H, Takebe Y (1999) Role of naturally occurring basic amino acid substitutions in the human immunodeficiency virus type 1 subtype E envelope V3 loop on viral coreceptor usage and cell tropism. J Virol 73: 5520–5526.
14. Simmonds P, Balfe P, Ludlam CA, Bishop JO, Brown AJ (1990) Analysis of sequence diversity in hypervariable regions of the external glycoprotein of human immunodeficiency virus type 1. J Virol 64: 5840–5850.
15. Bonhoeffer S, Holmes SE, Nowak M (1995) Causes of HIV diversity. Nature 376: 125.
16. Yamaguchi Y, Gojobori T (1997) Evolutionary mechanisms and population dynamics of the third variable envelope region of HIV within single hosts. Proc Natl Acad Sci U S A 94: 1264–1269.
17. Fouts TR, Binley JM, Trkola A, Robinson JE, Moore JP (1997) Neutralization of the human immunodeficiency virus type 1 primary isolate JR-FL by human monoclonal antibodies correlates with antibody binding to the oligomeric form of the envelope glycoprotein complex. J Virol 71: 2779–2785.
18. Parren PW, Mondor I, Naniche D, Ditzel HJ, Klasse PJ, et al. (1998) Neutralization of human immunodeficiency virus type 1 by antibody to gp120 is determined primarily by occupancy of sites on the virion irrespective of epitope specificity. J Virol 72: 3512–3519.
19. Moore JP, Cao Y, Qing L, Sattentau QJ, Pyati J, et al. (1995) Primary isolates of human immunodeficiency virus type 1 are relatively resistant to neutralization by monoclonal antibodies to gp120, and their neutralization is not predicted by studies with monomeric gp120. J Virol 69: 101–109.
20. Burton DR (1997) A vaccine for HIV type 1: the antibody perspective. Proc Natl Acad Sci U S A 94: 10018–10023.
21. Desrosiers RC (1999) Strategies used by human immunodeficiency virus that allow persistent viral replication. Nat Med 5: 723–725.
22. Stamatatos L, Cheng-Mayer C (1995) Structural modulations of the envelope gp120 glycoprotein of human immunodeficiency virus type 1 upon oligomerization and differential V3 loop epitope exposure of isolates displaying distinct tropism upon virion-soluble receptor binding. J Virol 69: 6191–6198.
23. Lusso P, Earl PL, Sironi F, Santoro F, Ripamonti C, et al. (2005) Cryptic nature of a conserved, CD4-inducible V3 loop neutralization epitope in the native envelope glycoprotein oligomer of CCR5-restricted, but not CXCR4-using, primary human immunodeficiency virus type 1 strains. J Virol 79: 6957–6968.
24. Bou-Habib DC, Roderiquez G, Oravecz T, Berman PW, Lusso P, et al. (1994) Cryptic nature of envelope V3 region epitopes protects primary monocytotropic human immunodeficiency virus type 1 from antibody neutralization. J Virol 68: 6006–6013.
25. Cavacini LA, Duval M, Robinson J, Posner MR (2002) Interactions of human antibodies, epitope exposure, antibody binding and neutralization of primary isolate HIV-1 virions. Aids 16: 2409–2417.
26. Chesebro B, Wehrly K, Nishio J, Perryman S (1992) Macrophage-tropic human immunodeficiency virus isolates from different patients exhibit unusual V3 envelope sequence homogeneity in comparison with T-cell-tropic isolates: definition of critical amino acids involved in cell tropism. J Virol 66: 6547–6554.
27. Milich L, Margolin B, Swanstrom R (1993) V3 loop of the human immunodeficiency virus type 1 Env protein: interpreting sequence variability. J Virol 67: 5623–5634.
28. Ida S, Gatanaga H, Shioda T, Nagai Y, Kobayashi N, et al. (1997) HIV type 1 V3 variation dynamics in vivo: long-term persistence of non-syncytium-inducing genotypes and transient presence of syncytium-inducing genotypes during the course of progressive AIDS. AIDS Res Hum Retroviruses 13: 1597–1609.
29. Sato H, Shiino T, Kodaka N, Taniguchi K, Tomita Y, et al. (1999) Evolution and biological characterization of human immunodeficiency virus type 1 subtype E gp120 V3 sequences following horizontal and vertical virus transmission in a single family. J Virol 73: 3551–3559.
30. Shiino T, Kato K, Kodaka N, Miyakuni T, Takebe Y, et al. (2000) A group of V3 sequences from human immunodeficiency virus type 1 subtype E non-syncytium-inducing, CCR5-using variants are resistant to positive selection pressure. J Virol 74: 1069–1078.
31. Robertson DL, Anderson JP, Bradac JA, Carr JK, Foley B, et al. (2000) HIV-1 nomenclature proposal. Science 288: 55–56.
32. Tajima F (1989) Statistical method for testing the neutral mutation hypothesis by DNA polymorphism. Genetics 123: 585–595.
33. Sato H, Kato K, Takebe Y (1999) Functional complementation of the envelope hypervariable V3 loop of human immunodeficiency virus type 1 subtype B by the subtype E V3 loop. Virology 257: 491–501.
34. Hachiya A, Aizawa-Matsuoka S, Tanaka M, Takahashi Y, Ida S, et al. (2001) Rapid and simple phenotypic assay for drug susceptibility of human immunodeficiency virus type 1 using CCR5-expressing HeLa/CD4(+) cell clone 1–10 (MAGIC-5). Antimicrob Agents Chemother 45: 495–501.
35. Pau CP, Lee-Thomas S, Auwanit W, George JR, Ou CY, et al. (1993) Highly specific V3 peptide enzyme immunoassay for serotyping HIV-1 specimens from Thailand. Aids 7: 337–340.
36. Sato H, Tomita Y, Ebisawa K, Hachiya A, Shibamura K, et al. (2001) Augmentation of human immunodeficiency virus type 1 subtype E (CRF01_AE) multiple-drug resistance by insertion of a foreign 11-amino-acid fragment into the reverse transcriptase. J Virol 75: 5604–5613.
37. Kusagawa S, Sato H, Tomita Y, Tatsumi M, Kato K, et al. (2002) Isolation and characterization of replication-competent molecular DNA clones of HIV type 1 CRF01_AE with different coreceptor usages. AIDS Res Hum Retroviruses 18: 115–122.
38. Zhu P, Liu J, Bess J Jr, Chertova E, Lifson JD, et al. (2006) Distribution and three-dimensional structure of AIDS virus envelope spikes. Nature 441: 847–852.
39. Chabot DJ, Chen H, Dimitrov DS, Broder CC (2000) N-linked glycosylation of CXCR4 masks coreceptor function for CCR5-dependent human immunodeficiency virus type 1 isolates. J Virol 74: 4404–4413.
40. Nei M, Gojobori T (1986) Simple methods for estimating the numbers of synonymous and nonsynonymous nucleotide substitutions. Mol Biol Evol 3: 418–426.
41. Ota T, Nei M (1994) Variance and covariances of the numbers of synonymous and nonsynonymous substitutions per site. Mol Biol Evol 11: 613–619.
42. Shannon CE (1997) The mathematical theory of communication. 1963. MD Comput 14: 306–317.
43. Rozas J, Sanchez-DelBarrio JC, Messeguer X, Rozas R (2003) DnaSP, DNA polymorphism analyses by the coalescent and other methods. Bioinformatics 19: 2496–2497.
44. Soda Y, Shimizu N, Jinno A, Liu HY, Kanbe K, et al. (1999) Establishment of a new system for determination of coreceptor usages of HIV based on the human glioma NP-2 cell line. Biochem Biophys Res Commun 258: 313–321.
45. Oka T, Yamamoto M, Yokoyama M, Ogawa S, Hansman GS, et al. (2007) Highly conserved configuration of catalytic amino acid residues among calicivirus-encoded proteases. J Virol 81: 6798–6806.
46. Song H, Nakayama EE, Yokoyama M, Sato H, Levy JA, et al. (2007) A single amino acid of the human immunodeficiency virus type 2 capsid affects its replication in the presence of cynomolgus monkey and human TRIM5alphas. J Virol 81: 7280–7285.
47. Case DA, Cheatham TE 3rd, Darden T, Gohlke H, Luo R, et al. (2005) The Amber biomolecular simulation programs. J Comput Chem 26: 1668–1688.
48. Peden K, Emerman M, Montagnier L (1991) Changes in growth properties on passage in tissue culture of viruses derived from infectious molecular clones of HIV-1LAI, HIV-1MAL, and HIV-1ELI. Virology 185: 661–672.

JOURNAL OF VIROLOGY, Apr. 2008, p. 3261–3270 Vol. 82, No. 7
0022-538X/08/$08.00+0 doi:10.1128/JVI.01154-07

Amino Acid Mutation N348I in the Connection Subdomain of Human Immunodeficiency Virus Type 1 Reverse Transcriptase Confers Multiclass Resistance to Nucleoside and Nonnucleoside Reverse Transcriptase Inhibitors▽†

Atsuko Hachiya,[1,2] Eiichi N. Kodama,[3]* Stefan G. Sarafianos,[4] Matthew M. Schuckmann,[4] Yasuko Sakagami,[3] Masao Matsuoka,[3] Masafumi Takiguchi,[2] Hiroyuki Gatanaga,[1] and Shinichi Oka[1]

AIDS Clinical Center, International Medical Center of Japan, Tokyo, Japan[1]; Center for AIDS Research, Kumamoto University, Kumamoto, Japan[2]; Institute for Virus Research, Kyoto University, Kyoto, Japan[3]; and Department of Molecular Microbiology and Immunology, University of Missouri School of Medicine, Bond Life Sciences Center, Columbia, Missouri[4]

Received 28 May 2007/Accepted 9 January 2008

We identified clinical isolates with phenotypic resistance to nevirapine (NVP) in the absence of known nonnucleoside reverse transcriptase inhibitor (NNRTI) mutations. This resistance is caused by N348I, a mutation at the connection subdomain of human immunodeficiency virus type 1 (HIV-1) reverse transcriptase (RT). Virologic analysis showed that N348I conferred multiclass resistance to NNRTIs (NVP and delavirdine) and to nucleoside reverse transcriptase inhibitors (zidovudine [AZT] and didanosine [ddI]). N348I impaired HIV-1 replication in a cell-type-dependent manner. Acquisition of N348I was frequently observed in AZT- and/or ddI-containing therapy (12.5%; $n = 48$; $P < 0.0001$) and was accompanied with thymidine analogue-associated mutations, e.g., T215Y ($n = 5/6$) and the lamivudine resistance mutation M184V ($n = 1/6$) in a Japanese cohort. Molecular modeling analysis shows that residue 348 is proximal to the NNRTI-binding pocket and to a flexible hinge region at the base of the p66 thumb that may be affected by the N348I mutation. Our results further highlight the role of connection subdomain residues in drug resistance.

Combinations of multiple drugs used for clinical treatment of human immunodeficiency virus type 1 (HIV-1) infections in highly active antiretroviral therapies (HAART) can dramatically reduce viral load, increase levels of CD4positive cells, improve survival rates, and delay the onset of AIDS. HAART typically includes two nucleoside reverse transcriptase inhibitors (NRTIs) and a nonnucleoside reverse transcriptase inhibitor (NNRTI) or a protease inhibitor (17). After prolonged therapy, however, an increasing number of treatment failures are caused by the emergence of multidrug-resistant (MDR) variants. For example, treatment with zidovudine (AZT) and dideoxynuleoside RT inhibitors such as didanosine (ddI) may result in the "Q151 complex" of clinical mutations in RT (A62V/V751/F77L/F116Y/Q151M) which causes high-level resistance to multiple NRTIs, AZT, ddI, zalcitabine (ddC), and stavudine (d4T) (21, 38). Another MDR complex of RT mutations is the "fingers insertion" complex that includes an insertion of two residues at the fingers subdomain of the p66 subunit of RT in the presence of AZT resistance mutations, e.g., M41L and T215Y (M41L/T69SSG/T215Y). This complex can emerge during combination treatment that includes NRTIs (10, 41) and confers resistance to multiple drugs by enhancing the excision reaction that causes resistance by unblocking NRTI-terminated primers (40). G333E or G333D polymorphisms with thymidine analogue-associated mutations (TAMs) and M184V have also been reported to facilitate moderate resistance to at least two NRTIs, AZT and lamivudine (3TC) (7, 22). RT mutations K103N, V106M, and Y188L are associated with resistance to multiple NNRTIs (1, 5). Since all NNRTIs bind at the same hydrophobic binding pocket, mutations in the binding pocket may result in broad cross-resistance between members of this family of drugs.

The presence of variants that are resistant to multiple drugs limits significantly the available therapeutic strategies and, even more profoundly, therapeutic options. However, so far all reports of viruses that acquire resistance to members of both families of RT inhibitors describe variants with multiple mutations at several residues that confer either NRTI or NNRTI resistance. Recently, Paolucci et al. reported that Q145M/L mutations confer cross-resistance to some NRTIs and NNRTIs (31, 32). Similarly, an NNRTI resistance mutation, Y181I, also confers resistance to d4T at the enzyme level (2). The frequency of these mutations in clinical isolates does not appear to be significant, according to the Stanford HIV resistance database (http://hivdb.stanford.edu/index.html); there is no deposition for Q145M/L, and Y181I has a prevalence of 0.02% in drug-naïve or NRTI-treated patients and 0.9% in NNRTI-treated patients.

We report here that N348I is a multiclass resistance mutation involved in resistance to both NRTIs and NNRTIs and present in a significant number of clinical isolates. Residue 348 is at the RT connection subdomain outside the region usually

* Corresponding author. Mailing address: Laboratory of Virus Immunology, Research Center for AIDS, Institute for Virus Research, Kyoto University, 53, Kawaramachi, Shogoin, Sakyo-ku, Kyoto 606-8507, Japan. Phone and fax: 81 75 751 3986. E-mail: ekodama@virus.kyoto-u.ac.jp.

† Supplemental material for this article may be found at http://jvi.asm.org/.

▽ Published ahead of print on 23 January 2008.

sequenced as the drug resistance assay in clinical settings. The role of connection subdomain mutations in AZT resistance has been highlighted recently by Pathak and colleagues (28). The present work shows that N348I confers resistance not only to the NRTI AZT but also to another NRTI, ddI, and two NNRTIs, nevirapine (NVP) and delavirdine (DLV). Importantly, we show that the N348I variant emerges frequently during chemotherapy containing AZT and/or ddI. To our knowledge, this is the first example of a clinically significant and high-prevalence multiclass RTI resistance mutation that highlights the need for extensive phenotypic and genotypic assays to detect novel mutations with important implications on future therapeutic strategies.

MATERIALS AND METHODS

Reagents and cells. AZT, ddI, ddC, and d4T were purchased from Sigma (St. Louis, MO). 3TC, DLV, and tenofovir (TDF) were purchased from Moravek Biochemicals, Inc. (Brea, CA). NVP, abacavir (ABC), and efavirenz (EFV) were generously provided by Boehringer Ingelheim Pharmaceutics Inc. (Ridgefield, CT), GlaxoSmithKline (Philadelphia, PA), and Merck Co. Inc. (Rahway, NJ), respectively. Loviride was kindly provided by S. Shigeta, Fukushima Medical University (Fukushima, Japan). MT-2, SupT1, PM1, H9, Cos-7, and MAGIC-5 cells (CCR5-transduced HeLa-CD4/LTR-β-Gal cells) were cultured and used as described previously (14). Peripheral blood mononuclear cells (PBMCs) obtained from healthy donors were stimulated with phytohemagglutinin (PHA) for 3 days and grown in RPMI 1640 medium with 10% fetal calf serum and 10 U of interleukin-2 as described previously (15, 23).

Clinical isolates. Clinical isolates were obtained from fresh plasma of an HIV-1-infected patient attending the outpatient clinic of the AIDS Clinical Center, International Medical Center of Japan, using MAGIC-5 cells. The isolates were stored at −80°C until use, and infectivity was measured as blue cell-forming units (BFU) of MAGIC-5 cells. The Institutional Review Board approved this study (IMCJ-H13-80), and written informed consent was obtained from the patient.

Viruses and construction of recombinant HIV-1 clones. An HIV-1 infectious clone, pNL101, was kindly provided by K.-T. Jeang (NIH, Bethesda, MD) and used for generating recombinant HIV-1 clones (15). A wild-type (WT) HIV-1, designated HIV-1_{WT}, was constructed by replacing the *pol*-coding region (nucleotides [nt] 2006 of ApaI site to 5785 of SalI site of pNL101) with the HIV-1 BH10 strain. The *pol*-coding region contains a silent mutation at nt 4232 (TTTAGA to TCTAGA; mutation is italicized) for generation of an XbaI unique site. The DNA fragments amplified by reverse transcription-PCR from the primary isolates were digested with appropriate restriction enzymes and cloned into pNL-RT_{WT}. The nucleoside sequences of the PCR-amplified fragments were verified with a model 3730 automated DNA Sequencer (Applied Biosystems, Foster, CA). Viral stocks were obtained by transfection of each molecular clone into Cos-7 cells, harvested, and stored at −80°C until use.

Sequencing analysis of HIV-1 RT region. Viral RNA was extracted from plasma and/or culture supernatant of clinical isolates and subjected to reverse transcription-PCR using a OneStep RNA PCR Kit (Takara Bio, Otsu, Japan). Nested PCR was subsequently conducted for direct sequencing. Primer pairs used for amplification of the DNA fragment from nt 2574 to 3333 of pNL101 were T1 (5′-AGGGGGAATTGGAGGTTT; nt 2393 to 2410) and T4 (5′-TTCT GTTAGTGCTTTGGTT; nt 3422 to 3404) for the first PCR and T12 (5′-CCAG TAAAATTAAAGCCAG; nt 2574 to 2592) and T15 (5′-TCCCACTAACTTCT GTATGTC; nt 3335 to 3315) for the second PCR (15). Primer pairs used for amplification of DNA fragment from nt 3288 to 4316 were 3244F (5′-AT GAACTCCATCCTGACAAATG; nt 3244 to 3265) and 4428R (5′-TGTA CAATCTAATTGCCATAT; nt 4428 to 4407) for the first PCR and 3288F (5′-CCAGAAAAAGACAGCTGGACT; nt 3288 to 3308) and 4316R (5′-TG GCAGATTAAAATCACTAGCC; nt 4316 to 4295) for the second PCR (13). The nested PCR products were then subjected to the direct sequencing of the entire RT coding region, and some PCR products were further analyzed with clonal sequence determination as described previously (13, 15).

Drug susceptibility assay. HIV-1 sensitivity to various RTIs was determined in triplicate using MAGIC-5 cells as described previously (14). MAGIC-5 cells were infected with diluted virus stock (100 BFU) in the presence of increasing concentrations of RTIs, cultured for 48 h, fixed, and stained with X-Gal (5-bromo-4-chloro-3-indolyl-βD-galactopyranoside). The stained cells were counted under a light microscope. Drug concentrations reducing the cell number to 50% of that of the drug-free control (EC_{50}) were determined by referring to the dose-response curve.

Competition assay of HIV-1 replication. MT-2, SupT1, PM1, and H9 cells (2.5×10^5 cells/5 ml) and PHA-stimulated PBMCs (2.5×10^6 cells/5 ml) were infected with each virus preparation (500 BFU) for 4 h. The infected cells were then washed and cultured in a final volume of 5 ml. Culture supernatants (100 μl) were harvested from days 1 to 7 after infection, and the p24 antigen amounts were quantified (27).

Freshly prepared H9 cells (3×10^5 cells/well) were exposed to the mixture of viral preparations (300 BFU) and cultured to compare their replicative capacities, as previously described (15). On day 1 in culture, one-third of the infected H9 cells were harvested and washed twice with phosphate-buffered saline, followed by DNA extraction. Purified DNA was subjected to nested PCR to sequence the HIV-1 RT genes. The supernatant of the viral culture was transferred to uninfected H9 cells at 7-day intervals, and the cells harvested at each passage were subjected to direct DNA sequencing of the HIV-1 RT gene. Population change of the viral mixture was determined by the relative peak height on the sequencing electrogram. The persistence of the original amino acid substitution was confirmed in all infectious clones used in this assay.

Molecular modeling studies. The SYBYL and O programs were used to prepare molecular models of the complexes of WT and N348I HIV-1 RT with DNA, NVP, and the triphosphates of AZT and ddI. Starting atomic coordinates of HIV-1 RT in complex with DNA were obtained from the structures described by Tuske et al. (40), Sarafianos et al. (36), and Huang et al. (20) (Protein Data Bank [PDB] code numbers 1T05, 1N6Q, and 1RTD, respectively). Because there is no available structure of RT in complex with both NNRTI and DNA, we used structures of RT in complex with NNRTI to obtain initial coordinates of the NNRTI-binding pocket (9, 12). Specifically, we used the coordinates of the two β-sheets of the polymerase active site (β6-β9-β10 that contains the three catalytic aspartates and the YMDD motif as well as β12-β13 of the primer grip) to replace the corresponding regions in the RT-DNA complex. The N348I side chain mutation was manually modeled in the p66 subunit, and all structures were optimized using energy minimization protocols in SYBYL. The triphosphates of AZT and ddI were built based on the structures of AZT monophosphate and dTTP in PDB 1N6Q (36) and 1RTD (20) or of TDF diphosphate in the ternary complex of HIV-1 RT/DNA/TFV-DP, PDB 1T03 (40). The coordinate vector of the resulting structures was varied using a minimization procedure to minimize the potential energy by relieving short interatomic distances while maintaining structural integrity.

RESULTS

Resistance to NNRTIs observed in HIV-1 isolates. The clinical history of the patient is summarized in Fig. 1 and includes the variation of genotypic and phenotypic drug resistance profiles of sequential isolates with time (see also Table S1 and Fig. S1 in the supplemental material). In spite of the combination therapy, little immunologic and virologic response was observed; at time point 2, the CD4 count was 25/μl, and the plasma HIV-1 RNA levels were 2.1×10^6 copies/ml. However, no known drug resistance mutations associated to both NRTIs and NNRTIs were detected in the RT region at this point (Fig. 1B). Due to poor adherence, upon changing the regimen we observed only partial suppression of viral replication and limited increase in the CD4 count. TAMs with N348I accumulated during time points 3 to 6 (Fig. 1). In February 2000, the treatment was interrupted due to severe adverse effects, resulting in a rebound of viral load. In July 2000, the same therapy was resumed for approximately 1 year. No drug resistance-associated mutations were detected upon initiation of this therapy (time point 7). At time point 8, mixtures of two amino acid insertions at codon 69 with TAMs and N348I were detected, although these mutations disappeared after the treatment interruption at time point 10.

Interestingly, HIV-1 isolates at time points 5 and 6 showed resistance to NVP (44- and 25-fold, respectively) and to DLV

A

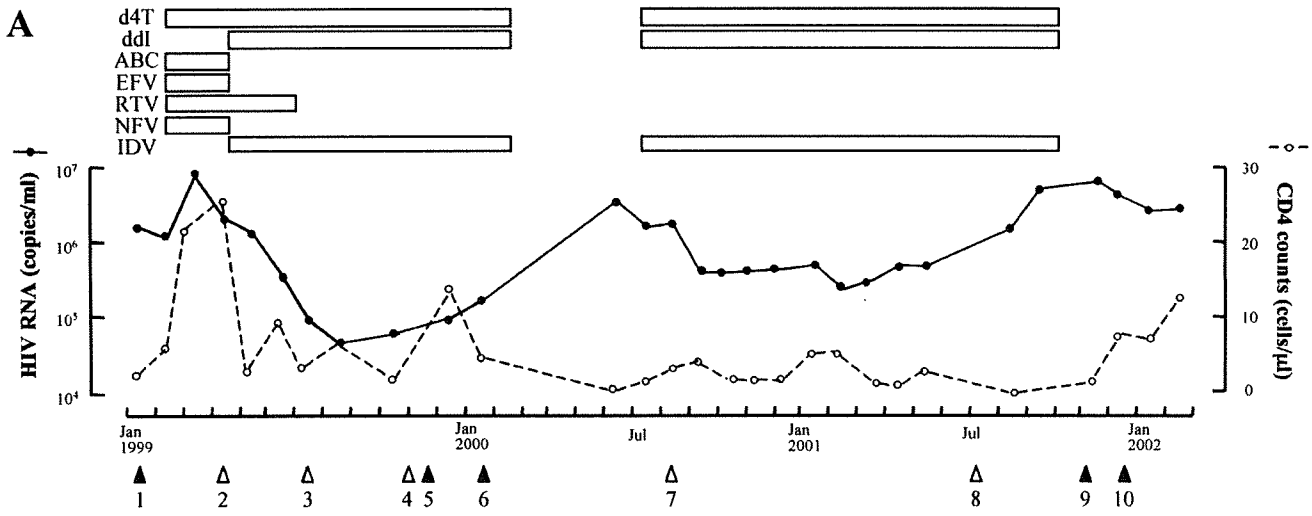

B

Time point	Resistance-associated and unique mutations												Fold increase in EC_{50}								
	M41	D67	T69	K70	V75	V118	L210	T215	L283	N348	I393		AZT	ddI	ddC	d4T	3TC	ABC	NVP	DLV	EFV
1	-	-	-	-	-	-	-	-	I	-	L		2	1.5	0.6	1.0	0.9	0.8	2.2	1	1
2	-	-	-	-	-	-	-	-	I	-	L						N.D.				
3	M/L	-	-	-	-	-	-	-	I	-	L						N.D.				
4	L	N	-	-	M	-	W	Y	I	N/I	L						N.D.				
5	L	N	-	-	M	-	W	Y	I	I	L		**44**	**4.3**	0.6	1.8	1.6	1.6	**44**	**8.5**	**3**
6	L	N	-	-	M	I	W	Y	I	I	L		**275**	**5.9**	2.5	**3.2**	**3.4**	2	**25**	**12**	1
7	-	-	-	-	-	-	-	-	I	-	L						N.D.				
8	L	T/N	-/SSG	E	M	I	W	Y	I	N/I	L						N.D.				
9	-	-	-	-	V/M	V/I	L/W	T/Y	I	-	-		2	1.2	0.6	1.1	0.6	1	2.4	1.5	0.7
10	-	-	-	-	-	-	-	-	I	-	-		2.8	0.7	0.6	1	0.8	1.2	1.8	1	1

FIG. 1. The course of patient and drug resistance profiles of clinical isolates obtained from the patient. (A) The drug treatment history is indicated at the top of the graph. The virologic responses represented by plasma viral load and CD4 counts of peripheral blood are shown. Open triangles indicate the time points of genotypic assays. Closed triangles indicate the time points of isolation of clinical isolates for genotypic assays (also see Fig. S1 in the supplemental material) and phenotypic assays (also see Table S1 in the supplemental material showing actual EC_{50} values as mean values and standard deviations from three independent experiments). From February to June 2000 and after October 2001, the chemotherapy was interrupted due to severe adverse effects. (B) The viruses acquired NRTI resistance mutations sequentially as shown. Susceptibility to compounds tested in at least three independent experiments is shown as the relative increase in the EC_{50} compared to HIV-1_{WT} obtained from a pNL4-3-based plasmid. An increase larger than 3.0-fold is indicated in bold. NRTI or NNRTI resistance mutations were reported in the HIV drug resistance database maintained by International AIDS Society 2006, the Stanford University (Stanford, CA) and Los Alamos National Laboratory (Los Alamos, NM), http://hivdb.stanford.edu/and http://resdb.lanl.gov/Resist_DB/, respectively. RTV, ritonavir; NFV, nelfinavir; IDV, indinavir.

(8.5- and 12-fold, respectively) but lacked any known NNRTI resistance-associated mutations except for L283I, which influences susceptibility of NNRTIs when combined with I135L/M/T (6) (Fig. 1B). However, L283I was detected at all points without I135L/M/T even in phenotypically sensitive viruses; therefore, it is unlikely that this single mutation is involved in the resistance. After the interruption at time points 9 and 10, the majority of HIV-1 detected in the plasma reverted to WT and was susceptible to all RTIs tested. The patient was previously treated with a regimen containing EFV, not NVP, for several months prior to the appearance of the N348I mutation. Importantly, this mutation was not detected in genotypic assays during treatment with EFV, but it was first detected 6 months after removal of EFV and use of ddI in the following regimen. Phenotypic and genotypic information at time point 5 shows that resistance to NVP and DLV was present while the patient was on a regimen that did not include any NNRTIs and in the absence of any known NNRTI resistance-related mutations. Thus, it is unlikely that the phenotypically identified NNRTI resistance in the patient was induced by the previous EFV-containing therapy.

RT C-terminal region confers NVP resistance. To identify the mutation(s) responsible for the resistance to NVP and DLV, we constructed chimeric clones with cDNA fragments of the RT region derived from the clinical isolates. Briefly, the N-terminal (amino acids 15 to 267) and C-terminal (amino acids 268 to 560) RT coding regions of clinical isolates were PCR amplified separately and used for replacement of the corresponding regions in the WT sequence of pNL-RT_{WT}. These chimeric clones were then examined for their susceptibility to RTIs (Table 1). Only the clones containing the C-terminal region derived from CL-6 isolated at time point 6 and

TABLE 1. Susceptibility of chimeric HIV-1 clones with N- and/or C-terminal RT region substitutions

RT-replaced region		EC_{50} (fold increase)[a]				
N terminus[b]	C terminus[c]	AZT	ddI	NVP	DLV	EFV
WT[d]	WT	0.038 ± 0.012	2.6 ± 1.04	0.05 ± 0.01	0.03 ± 0.01	0.003 ± 0.001
CL-6[e]	CL-6[e]	3.37 ± 0.97 (**89**)	14.3 ± 0.58 (**5.5**)	1.2 ± 0.21 (**24**)	0.16 ± 0.02 (**5.3**)	0.007 ± 0.004 (2.3)
CL-9[f]	CL-9[f]	0.04 ± 0.01 (1.1)	2.3 ± 1.21 (0.9)	0.13 ± 0.07 (2.6)	0.06 ± 0.02 (2)	0.004 ± 0.002 (1.3)
CL-6	WT	1.24 ± 0.34 (**33**)	4.6 ± 1.50 (1.8)	0.12 ± 0.06 (2)	0.04 ± 0.02 (1.3)	0.002 ± 0.001 (0.7)
WT	CL-6	0.19 ± 0.04 (**5**)	13.7 ± 2.31 (**5.3**)	1.67 ± 0.23 (**33**)	0.39 ± 0.06 (**13**)	0.006 ± 0.002 (2)
CL-6	CL-9	1.50 ± 0.95 (**39**)	5.9 ± 1.21 (2.3)	0.10 ± 0.05 (2)	0.04 ± 0.02 (1.3)	0.002 ± 0.001 (0.7)

[a] The data shown are mean values ± standard deviations obtained from the results of at least three independent experiments, and the relative increase in the EC_{50} values for recombinant viruses compared with WT is shown in parentheses. Bold indicates an increase in EC_{50} value greater than threefold relative to the WT.
[b] RT N-terminal region contains mainly the domains of finger and palm and partially thumb (amino acid positions 15 to 267).
[c] RT C-terminal region contains domains of thumb, connection, and RNase H (amino acid positions 268 to 560).
[d] DNA fragment is identical to pNL-RT_{WT}.
[e] N- and C-terminal regions of CL-6 contained T39A/M41L/K43E/D67N/V75M/V118I/I132V/L210W/T215Y and N348I/I393L in their coding regions, respectively (see also Fig. S1 in the supplemental material).
[f] No resistance-associated mutations were observed in either the N- or C-terminal region of CL-9 (also see Fig. S1 in the supplemental material).

showed resistance (Fig. 1; see also Fig. S1 in the supplemental material) to NVP and DLV. Interestingly, the C-terminal region also conferred resistance to AZT and ddI even in the absence of AZT resistance mutations that normally reside at the N-terminal region within amino acids 41 to 219. Recently, mutations in the connection subdomain, including G335D, N348I, and A360T, have been shown to confer AZT resistance (28). In these clinical isolates the C-terminal region contained four unique mutations in the connection subdomain: G335D, N348I, A360T, and I393L (see Fig. S1 in the supplemental material). G335D and A360T were continuously observed at every time point and are polymorphisms related to subtype D. Since these isolates showed no phenotypic resistance (Table 1 and Fig. 1B), it is unlikely that G335D and A360T are involved in the resistance, at least in subtype D. I393L was also continuously detected from time point 1 but disappeared after the treatment interruption at time point 9 (Fig. 1) while N348I appeared only from time points 4 to 6 and at point 8 under treatment.

To further clarify the effect of mutations at residues 348 and 393 on drug resistance, we generated the N348I and/or I393L mutations in the C-terminal region by site-directed mutagenesis on a pNL-RT_{WT} background. Consistent with the phenotypic experiments and the experiments with chimeric viruses, we found that the N348I substitution conferred resistance to AZT, ddI, NVP, and DLV. In contrast, we found that the I393L mutation caused no significant resistance by itself (Table 2). Furthermore, the combination of I393L with N348I did not show any significant increase in NVP resistance compared to N348I alone.

To address whether N348I further increases the level of AZT resistance in the presence of TAMs, we examined the effect of N348I on AZT susceptibility in the presence or absence of the classical AZT resistance mutations M41L/T215Y. M41L/T215Y or N348I showed only moderate resistance to AZT whereas a combination of M41L/T215Y and N348I further enhanced AZT resistance (Table 2). These data demonstrate that the N348I mutation is responsible for this cross-resistance to multiple members of the NRTI and NNRTI families and enhances AZT resistance induced by TAMs.

Viral replication kinetics. Since N348I and I393L immediately disappeared after cessation of HAART, we examined whether these mutations have an effect on viral replication kinetics using the p24 antigen production assay and a competitive HIV-1 replication assay (CHRA). In the p24 antigen production assay, acquisition of N348I drastically impaired replication in MT-2 and SupT1 cells (Fig. 2A and B). However, a moderately low reduction of replication kinetics was observed in PM1, H9 cells, and PHA-stimulated PBMCs (Fig. 2C, D, and E). HIV-1 carrying the mutation I393L (HIV-1_{I393L}) showed comparable replication kinetics in all cells tested. A combination of I393L with N348I showed no apparent change of replication kinetics in MT-2, SupT1 cells, and PHA-stimulated PBMCs (Fig. 2A, B, and E) and reduction in PM1 cells (Fig. 2C) compared to N348I alone. CHRA was performed for further comparison of replication kinetics in H9 cells. During 6 weeks in culture, we observed little difference in viral replication in H9 cells (Fig. 2F). A lack of an effect of I393L on the replication of N348I was confirmed by CHRA (Fig. 2G). These results indicate that N348I impairs viral replication in a cell-type-dependent manner and that I393L exerts little effect on viral replication of either the WT or N348I clones. Thus, I393L appears to be one of the specific polymorphisms for this isolate.

Insertion at 69 and N348I. At time point 8 we detected the transient presence of the fingers insertion mutation, a 2-amino-acid insertion at codon 69 in the presence of TAMs known to confer resistance to NRTIs by enhancing the excision reaction (3) (Fig. 1). Interestingly, at time point 8 WT N348 coexisted with resistant I348. To address whether these two MDR mutations were introduced onto the same RNA genome, we carried out clonal sequence analysis of PCR products. The results show that the fingers insertion and the N348I mutations were randomly introduced; seven, three, one, and six clones ($n = 17$) contained both mutations, the fingers insertion only, N348I only, and no mutation or insertion, respectively, in the background of TAMs (Table 3). In previous studies the fingers insertion complex emerged with the K70E mutation that was selected in vitro with adefovir (8) and β-2′,3′-didehydro-2′,3′-dideoxy-5-fluorocytidine (18), and it conferred low level resistance to TDF, ABC, and 3TC (39). The effect of K70E on resistance or enzymatic activity influenced by the fingers insertion remains to be elucidated. These results suggest that there is no correlation between the N348I and the

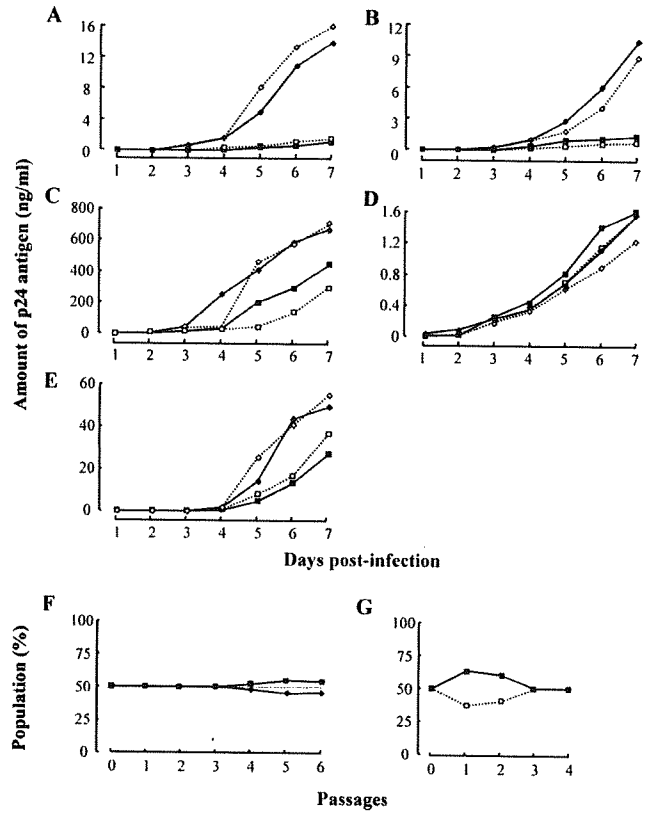

FIG. 2. Viral replication kinetics. Production of p24 antigen in culture supernatant was determined with a commercially available p24 antigen kit. Profiles of replication kinetics (p24 production) of HIV-1_{WT} (closed diamonds), HIV-1_{N348I} (closed squares), HIV-1_{I393L} (open diamonds) and HIV-$1_{N348I/I393L}$ (open squares) were determined with MT-2 (A), SupT1 (B), PM1 (C) and H9 cells (D) and PHA-stimulated PBMCs (E). Representative results from at least two (or three) independent single determinations of p24 production with newly titrated viruses are shown. A competitive HIV-1 replication assay was performed in H9 cells to compare the replication kinetics of HIV-1_{WT} (closed diamond) and HIV-1_{N348I} (closed squares) (F) and of HIV-1 N348I (closed squares) and HIV-$1_{N348I/I393L}$ (open square) (G).

finger insertion mutations. Because our studies show that N348I does not confer d4T resistance, we speculate that the fingers insertion mutation was introduced to overcome the drug pressure by d4T.

TABLE 3. Sequences of HIV-1 RT-coding region of clinical samples

No. of clones[a]	Resistance-associated and unique mutation at the indicated position									
	M41	D67	T69	K70	V75	V118	L210	T215	N348	I393
5	L	N			M	I	W	Y		L
3	L	T	SSG	E	M		W	Y	I	L
3	L	T	SSG	E	M	I	W	Y	I	L
2	L	T	SSG	E			W	Y		L
1	L	T	SSG	E			W	Y	I	L
1	L	T	SSG	E	M	I	W	Y		L
1	L				M					
1	L				M	I	W	Y	I	L

[a] The PCR product at time point 8 was subcloned and sequenced (n = 17).

TABLE 2. Drug susceptibilities of HIV-1 variants constructed by site-directed mutagenesis

Mutation[a]	EC_{50} (fold increase)[b]											
	NRTI							NNRTI				
	AZT	ddI	ddC	d4T	3TC	ABC	TDF	NVP	DLV	Loviride	EFV
WT	0.035 ± 0.01	2.3 ± 0.14	0.7 ± 0.13	3.6 ± 1.36	2.1 ± 0.2	3.4 ± 0.14	0.03 ± 0.01	0.04 ± 0.02	0.04 ± 0.01	1.4 ± 0.38	0.003 ± 0.0008
N348I	0.24 ± 0.04 (**6.9**)	12 ± 1.0 (**5.2**)	0.74 ± 0.58 (1.1)	2.9 ± 0.21 (0.8)	1.7 ± 0.36 (0.8)	3.4 ± 1.11 (1)	0.02 ± 0.01 (0.7)	1.07 ± 0.06 (**27**)	0.22 ± 0.04 (**5.5**)	2.4 ± 0.35 (1.7)	0.005 ± 0.0005 (1.7)
I393L	0.06 ± 0.01 (1.7)	2 ± 1.37 (0.9)	0.42 ± 0.23 (0.6)	1.8 ± 1.21 (0.5)	1.5 ± 0.74 (0.7)	2.4 ± 0.95 (0.7)	0.02 ± 0.01 (0.7)	0.05 ± 0.01 (1.3)	0.04 ± 0.01 (1.0)	2.2 ± 0.4 (1.6)	0.003 ± 0.001 (1)
N348I/I393L	0.23 ± 0.03 (**6.6**)	11.3 ± 1.53 (**4.9**)	0.49 ± 0.01 (0.7)	4.2 ± 1.12 (1.2)	1.7 ± 0.40 (0.8)	2.7 ± 0.26 (0.8)	0.02 ± 0.01 (0.7)	1.02 ± 0.51 (**26**)	0.28 ± 0.06 (**7**)	2.6 ± 0.42 (1.8)	0.005 ± 0.001 (1.7)
M41L/T215Y	0.28 ± 0.06 (**8**)	4.5 ± 1.55 (2)	ND	ND	1.3 ± 0.25 (0.6)	ND	ND	0.05 ± 0.01 (1.3)	0.04 ± 0.02 (1)	ND	0.002 ± 0.0004 (0.7)
M41L/T215Y/ N348I	1.37 ± 0.21 (**39**)	9.9 ± 0.99 (**4.3**)	ND	ND	1.4 ± 0.20 (0.7)	ND	ND	1.11 ± 0.69 (**28**)	0.15 ± 0.06 (**3.8**)	ND	0.002 ± 0.0004 (0.7)

[a] See Materials and Methods for the construction of clones.

[b] Data are means ± standard deviations from at least three independent experiments. The relative increase in the EC_{50} value compared with that in HIV-1_{WT} is given in parentheses. Boldface indicates an increase greater than threefold. ND, not determined.

TABLE 4. Frequency of N348I acquisition in clinical isolates

Treatment group	No. of isolates (%)		*P* value[a]
	Total in group	With N348I	
AZT and/or ddI	48	6 (12.5)	<0.0001
AZT	22	2 (9.1)	0.011
ddI	16	2 (12.5)	0.006
AZT/ddI	10	2 (20)	0.002
Control	183	0	
Antiretrovirals with neither AZT nor ddI	55	0	
No antiretrovirals	128	0	
Deposited in Los Alamos database	328	3 (0.9)	0.0002

[a] The *P* value was determined by the Fisher's exact test. For the AZT and/or ddI treatment groups, values were compared with the control group. The P value for isolates deposited in the Los Alamos database was determined based on a comparison with the AZT and/or ddI treatment group.

Prevalence of N348I. We obtained viral specimens from 231 infected patients who visited our clinical center from May 1997 to July 2003 and analyzed HIV-1 sequences by direct sequencing (Table 4). The viral specimens were classified in two groups: (i) those from patients treated with AZT and/or ddI (n = 48) and (ii) those from patients treated by regimens with neither AZT nor ddI (control group, n = 183). The group treated with AZT and/or ddI was further divided into three subgroups based on the treatment received: with AZT, with ddI, and with the AZT/ddI combination (Table 4). During chemotherapy containing AZT (n = 22), ddI (n = 16), or the combination of AZT and ddI (n = 10), two patients each harbored HIV-1 with the N348I mutation. Acquisitions of N348I in all of the subgroups was statistically significant (P = 0.011, 0.006, and 0.002, respectively). In contrast, none of the patients in the control group (n = 183) harbored N348I variants. Only three variants with N348I are deposited in the Los Alamos HIV sequence database that includes subtypes B, D, and CRF14 (http://www.hiv.lanl.gov/content/hiv-db/mainpage.html). Thus, prevalence of N348I was statistically significant in the group treated that received chemotherapy containing AZT and/or ddI (P < 0.0001).

Because at present the numbers of NVP- or DLV-containing regimens without AZT and/or ddI are limited in our cohort (n = 6 or n = 0, respectively), we were not able to detect acquisition of N348I in these groups. Acquisition of N348I was observed in two patients treated with EFV (Table 5). Notably, these two patients were simultaneously treated with AZT and ddI, suggesting that the significance of EFV treatment for the emergence of N348I remains unknown.

Profiles of patients infected with HIV-1 containing the N348I mutation. We further analyzed the profiles of HIV-1

TABLE 5. Profiles of patients infected with HIV-1 containing the N348I mutation

Patient	Subtype of RT region[a]	Antiretroviral treatment	Duration (mo)	HIV RNA (copies/ml)	N348I	RT mutation(s) by region	
						Polymerase subdomain	Connection subdomain[d]
Case 1[b]	D	d4T, ddI, IDV	6	6.1×10^4	+/−	M41L, D67N, V75M, L210W, T215Y	G335D, A360T
		d4T, ddI, IDV	7	ND[c]	+	M41L, D67N, V75M, L210W, T215Y	G335D, A360T
Case 2	B	AZT, ddC, NFV	1	7.9×10^3	−		A360T
		AZT, ddC, NFV	4	9×10^3	−		A360T
		AZT, ddC, NFV	6	1.2×10^4	+/−	T215N/S/Y	A360T
		AZT, ddC, NFV	10	3.5×10^4	+	D67N, K70R, T215Y[e]	A360T
		d4T, 3TC, RTV, SQV	8	<50	ND	ND	ND
Case 3	B	AZT, 3TC, RTV, SQV	7	3.5×10^5	−		A360T, A376T
		AZT, 3TC, RTV, SQV	8	1.9×10^5	+	M41L, D67N, T69D, M184V, L210L/W, T215Y	A360T, A376T
		None (interruption)	7	1.2×10^5	+	M41L, D67N, T69D, M184M/V, L210L/W, T215Y	A360T, A376T
		ABC, EFV, RTV	3	60	ND	ND	ND
Case 4	B	AZT, 3TC, ddI, EFV	3	1.7×10^3	+	M184V	
Case 5	B	d4T, ddI, RTV, SQV	23	9.9×10^3	+	M41L, L210W, T215Y	
		AZT, ddI, RTV, SQV	3	6.3×10^4	+	M41L, T69D, L210W, T215Y, K219R	
		None (interruption)	7	1.8×10^5	−		
		ABC, TDF, LPV, EFV	7	<50	ND	ND	ND
Case 6	B	AZT, ddI, EFV	3	180	−		ND
		AZT, ddI, EFV	5	540	+/−	T215T/Y	ND
		AZT, ddI, EFV	6	1.1×10^4	+	T215Y	
		None (interruption)	2	2.4×10^5	−		
		d4T, 3TC, LPV	8	<50	ND	ND	ND

[a] The RT regions were sequenced and subjected to subtype analysis (http://www.ncbi.nlm.nih.gov/projects/genotyping/formpage.cgi).
[b] This patient is described in this study.
[c] ND, not detectable.
[d] G335D is an observed polymorphism in subtype D. A360I/V and A376S were reported to be AZT-resistant mutations (24).
[e] Phenotype assays were performed at 10 months for a regimen combining ddC, AZT, and NFV; resistance to AZT, ddI, and NVP was induced 52-, 6.8-, and 8.3-fold, respectively.

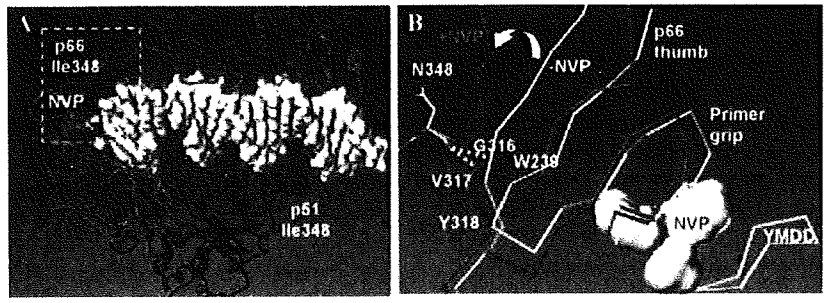

FIG. 3. Location of N348I in the modeled HIV-1 RT with NVP. (A) The N348I mutation (blue Van Der Waals volume) is shown in the connection subdomains of both p66 (purple) and p51 (cyan) subunits. The 348 residue of the p51 subunit is distant from the nucleic acid, shown as yellow Van Der Waals surfaces. In the p66 subunit (purple) the 348 residue is in a position to affect the flexibility of the p66 thumb, which in turn might affect binding of the nucleic acid. NVP is shown bound at the NNRTI binding pocket (red Van Der Waals volume). Magnification of the frame area of the enzyme is shown in panel B. (B) The main chain C=O of N348 is shown to interact with the N-H of 317 (yellow broken line) through a hydrogen bond interaction. Binding of NVP (white ball) repositions the p66 thumb subdomain with respect to (i) the polymerase active site (β6-β9-β10) that contains the three catalytic aspartates and the YMDD motif and (ii) the primer grip (β12-β13) of p66. The movement of the thumb subdomain is in a hinge-like motion that is based at the position where residue 348 interacts with residue 317.

with N348I from the six infected patients described in Table 4. The results of this analysis are shown in Table 5. The RT regions were sequenced and subjected to analysis with the software Genotyping, which uses the BLAST algorithm to determine homologies with known subtypes (http://www.ncbi.nlm.nih.gov/projects/genotyping/formpage.cgi). HIV-1 variants in case 1 belonged to subtype D, and the others belonged to subtype B. All six patients received therapy containing AZT and/or ddI. Among them, two patients (cases 4 and 6) were under therapy with EFV. However, none of them was treated with NVP or DLV. The five N348I-containing variants were in the presence of TAMs that emerged during the therapies. TAMs in case 1 and some TAMs (M41L, L210W, and T215Y) in case 5 seemed to be induced by d4T, not by AZT. In case 3, the 3TC resistance mutation M184V that attenuates TAM-induced AZT resistance (24) was present together with N348I. Similarly, in case 4, M184V may confer AZT hypersusceptibility. In case 6, N348I was present together with a classical AZT resistance mutation, T215Y. Thus, except for case 5, even under AZT-containing therapy, the HIV-1 resistance level to AZT and ddI seemed to be intermediate and weak, respectively. Additionally, viral load in cases 2, 3, 5, and 6 dramatically decreased after introduction of a new regimen without AZT and/or ddI. These results indicated that N348I may enhance AZT resistance and at least act as a primary mutation for ddI.

In these six patients, HIV-1 with the G335D mutation was observed only in case 1. In the Los Alamos HIV sequence database, G335D has been observed in 77% of subtype D HIV-1 isolates (n = 35). A360T was detected in two isolates of subtype B and one isolate of subtype D and was observed in 13 and 51% of drug-naïve isolates of subtypes B and D, respectively. This suggests that A360T is also one of the polymorphisms. The A360V or A360I mutation has been reported to have a modest effect on AZT resistance (28). Meanwhile, none of N348I-containing subtype B variants (n = 5) had mutations associated with AZT resistance in the connection subdomain (28) (Table 5).

Molecular modeling. Residue 348 is located close to the hinge site of the thumb subdomain. Mutations at the virus level affect both subunits of RT. Figure 3 shows that residue 348 of the p51 subunit is located remotely from the polymerase active site (~60 Å) and from the NNRTI binding pocket (~55 Å). Furthermore, it is not in close proximity to the interface of the two subunits (~20 Å) or the DNA in the nucleic acid binding cleft (~15 Å). On the other hand, residue 348 of the p66 subunit is proximal to the NNRTI-binding site and the nucleic acid binding cleft. These relative distances suggest that it is more likely that the interactions involve mainly residue 348 of the p66 subunit. Subunit-specific biochemical analysis would determine the precise contribution of the N348I mutation in each subunit to the drug resistance phenotype. In the p66 subunit, the main chain of the 348 residue interacts through a hydrogen bond with the main chain of V317 of the p66 thumb subdomain (Fig. 3). To determine the degree of flexibility of this part of the structure of RT, we superposed 23 structures of RT complexes. The comparison revealed measurable differences. The length of the amide bond between the main chain C=O of residue 348 and N-H of V317 varies considerably (from 2.5 to 3.6 Å), suggesting a flexibility at the junction of the connection, thumb, and palm subdomains. It is likely that the N348I mutation affects the interactions of this residue with a number of neighboring residues. In the RT/DNA/deoxynucleoside triphosphate or RT/DNA/TDF structures of ternary catalytic complexes (PDB code 1RTD or 1T05, respectively), the change of N348 to a more hydrophobic Ile would improve the hydrophobic interactions with T351 of the p66 connection subdomain and with G316 and I270 of the p66 thumb subdomain. In other structures of complexes of RT with various NNRTIs (PDB codes 1S1X, 1S6P, 1S1U, 1S1T, 1S1W, 1TKZ, 1TKX, 1TL1, 1SUQ, 1SV5, 1HNI, 1HQU, and 1HNV), residue W239 appears to be in the vicinity of these residues and likely to be affected directly or indirectly by the N348I mutation. Notably, residue W239 interacts through P-P interactions with Y318, which has been involved in resistance to NNRTIs (NVP and DLV) (19, 33).

DISCUSSION

Two previous reports have shown that two rare mutations, Q145M/L and Y181I, can confer cross-resistance to some NRTIs and NNRTIs (31, 32). N348I appears to be the first reported high-prevalence amino acid mutation to confer resistance to multiple members of the NRTI and NNRTI families. N348 is highly conserved in HIV-1 strains, including subtype O. Interestingly, the equivalent residue in HIV-2 and other retroviruses is an isoleucine (Los Alamos Sequence Data Base, http://hiv-web.lanl.gov/content/hiv-db/). Similarly, WT HIV-2 RT resembles NNRTI-resistant HIV-1 RTs at the NNRTI binding pocket region, e.g., V/I at 181 and L at 188 (34). Any of these differences from the HIV-1 enzyme, including N348I, may contribute to the observed NNRTI resistance of the HIV-2 RT. The significance and role of I348 in the natural resistance of HIV-2 to NNRTIs and susceptibility to NRTIs remain to be elucidated by further experiments.

Recently, Shafer et al. proposed criteria for evaluating the relevance of mutations to drug resistance based on extensive resistance surveillance data (37). In this review the mutations related to drug resistance were assessed by the following: (i) correlations between a mutation and treatment (whether the drug therapy selects for the mutation), (ii) correlations between a mutation and decreased in vitro drug susceptibility, and (iii) correlations between a mutation and a diminished in vivo virologic response to a new antiretroviral regimen.

Regarding the first criterion, we showed that the N348I mutation was induced by AZT and/or ddI treatment (Table 4). For the second criterion, we showed that N348I decreases susceptibility to AZT, ddI, NVP, and DLV (Table 2). The AZT and ddI resistance of the N348I clone was comparable to that of M41L/T215Y and L74V, respectively. Additionally, N348I showed 27-fold increased resistance to NVP. Regarding the third criterion, our data on patient viral load levels shown in Table 5 indicate that N348I affected the clinical outcome. Specifically, in case 6, the viral load clearly increased upon acquisition of N348I. Moreover, dramatic decreases in viral load were observed after introduction of a new regimen without AZT and/or ddI, especially in cases 2, 3, 5, and 6. Hence, the N348I mutation meets the accepted criteria for being a drug resistance mutation.

At present, it is not possible to accurately compare the incidence of N348I with that of other resistance mutations. Genotypic analysis of the largest and most recent drug resistance surveillance examined 6,247 patients treated with well-characterized RTIs, mainly performed within amino acids 1 to 240 of the RT region (35). In this surveillance, the incidences of the Q151M complex and fingers insertion were 2.6 and 0.5%, respectively. Because the connection subdomain is located outside the region sequenced in the majority of genotypic assays, only limited data are available for connection subdomain mutations such as G333E/D and N348I. Nonetheless, the incidence of N348I in our cohort is higher than other MDR mutations such as that of the Q151M complex and the insertion mutations. Furthermore, prevalence of N348I in a Canadian cohort (11.3%) (42) is comparable to that in our Japanese cohort.

In the patient case presented in Fig. 1, there is strong evidence that N348I was not present during and at least 6 months after cessation of NNRTI-based therapy. Still, because of the limited number of such cases in our cohort, it remains unclear if N348I can be induced by NNRTI-containing regimens. According to the Stanford HIV drug resistance database, the incidence of N348I in patients treated with NNRTIs is 5.8% (n = 13/224), significantly higher than in the untreated group (0.1%; n = 2/1095, $P < 0.0001$). We report here that N348I confers significant and moderate resistance to NVP and DLV, respectively. Most recently, Yap et al. also reported that combined treatment with AZT and NVP was associated with increased risk in the emergence of N348I (42). They mention that other mutations, e.g., K103N, may further enhance N348I-induced resistance to EFV. Thus, it is possible that HIV-1 also acquires N348I under NNRTI-containing therapy. Further experiments and surveillance are needed in patients treated with NNRTI(s) as well as NRTIs.

Mutations at multiple residues are present in the MDR variants of the Q151M and the fingers insertion complexes. Q151M complexes typically contain at least four mutations, including V75I, F77L, and F116Y in addition to Q151M (21). Insertion complexes generally contain an insertion of six bases that code for two amino acids in the background of the classical AZT resistance backbone such as T215Y (41). These results suggest that genetic barriers to developing these MDR mutations appear to be high, consistent with their low incidence (35). Genetic barriers to the G333D/E complex also seem to be high, since G333D/E requires other TAMs to develop this certain resistance phenotype (7). In contrast, a single nucleotide substitution (AAT to ATT) is sufficient to develop the N348I mutation, indicating that the genetic barrier to N348I is low. This may contribute to an increased prevalence of N348I during prolonged chemotherapy with AZT and/or ddI.

The disappearance of N348I was relatively rapid following interruption of treatment (Fig. 1 and Table 5). This was consistent with the observed replication kinetics of N348I HIV-1 where strong impairment was observed in MT-2 and SupT1 cells (Fig. 2). However, in PM1 cells and PHA-stimulated PBMCs, this reduction was moderate, and in H9 cells little reduction was observed. Since both PM1 and H9 cells were originally derived from the same T-cell line, Hut78 (25, 26), some properties for HIV replication may be identical. Availability of deoxynucleoside triphosphates or some cellular factors may compensate the effect of N348I on RT activity, suggesting that some cell populations in patients might harbor HIV-1 with N348I due to its comparable replication kinetics with the WT.

How might the N348I mutation affect resistance to NRTI and NNRTI inhibitors that act with entirely different mechanisms and target different binding sites? Theoretically, it is possible that the N348I mutation at either p66 or p51 or both subunits is responsible for the resistance phenotype. It is also possible that NRTI and NNRTI resistance do not involve the same subunit. However, the N348I mutation in p51 is 50 to 60 Å away from the polymerase active site and the NNRTI binding pocket where the affected inhibitors are expected to bind. Similarly, the mutation site in p51 is 15 to 20 Å away from the interface of the two subunits or the DNA binding cleft. Meanwhile, the mutation site in the p66 subunit is close to the NNRTI-binding pocket and the nucleic acid binding cleft. Hence, it is more likely that the effects of the N348I mutation

are mediated through the p66 subunit mutation, although an involvement of the mutation at the p51 subunit currently cannot be ruled out and should be addressed by biochemical experiments.

In terms of NNRTI resistance, our molecular modeling analysis is consistent with a hypothesis that the mutation is likely to affect the flexibility and mobility of the p66 thumb subdomain. Extensive crystallographic work with HIV-1 RT in several forms, including an unliganded form, in complex with DNA substrates or NNRTIs has revealed that during the course of DNA polymerization, the p66 thumb subdomain undergoes major conformational motions that are critical for efficient catalysis. Alignment of multiple structures of HIV RT suggests that the p66 thumb moves as a rigid body with its base hinged to the palm subdomain exactly near residue 348 (Fig. 3). Residue 348 is proximal to, and likely to affect, the relative interactions between residues of the p66 connection (T351) and p66 thumb subdomains (V317, I270, P272, W239, and eventually Y318). The proximity of residue 348 to this hinge region leads us to believe that changes imparted by the N348I mutation alter the mobility and flexibility of the thumb subdomain. Subtle changes in the interactions between V317 and N348 may also reposition W239 and its neighboring Y318 in the NNRTI-binding pocket. Interestingly, the Y318F mutation affects NNRTI resistance in a similar way as N348I: it decreases susceptibility to NVP and DLV but not to EFV (19, 33). Biochemical binding experiments of RTs with NNRTIs would directly evaluate this hypothesis.

The effect of the N348I mutation on NRTI resistance cannot be rationalized by direct interactions of the mutated residue with the NRTI binding site. It is tempting to speculate that minor changes in the p66 thumb subdomain hinge motions also have minor effects on the positioning of the nucleic acid, which in turn affects the ability to discriminate between NRTI and the normal substrate by an as yet undefined mechanism. However, direct biochemical experimental evidence will be needed to determine the precise molecular details of the specific mechanisms of NRTI resistance.

It has been proposed previously that an imbalance between reverse transcription and RNA degradation plays an important role in NRTI resistance (25). Pathak and colleagues proposed that connection subdomain mutations may result in a slower RNase H reaction, and this in turn may provide an increased time period available for AZT excision, especially with TAMs (28–30). In the case of N348I, Yap et al. recently reported that N348I decreases RNase H enzymatic activity (42). At present, available evidence is consistent with a model in which these connection subdomain mutations alter the affinity of the RT for template/primer, enhance nucleoside excision, and reduce template switching.

Several studies, including recent work by Delviks-Frankenberry et al. and Brehm et al. (4, 11), highlighted the necessity to expand sequencing analysis to include the connection and RNase H subdomains. This contention is further supported by results in this work and by others (16, 28, 42, 43) showing that mutations at the connection subdomain influence susceptibility to some antiretroviral drugs. Hence, there is a growing interest in obtaining genotypic information from expanded areas of RT that would be useful for a more complete analysis of HIV drug resistance. Interestingly, already two out of four commercially available genotypic and phenotypic assay kits are designed to include in their analysis at least part of the connection subdomain (Antivirogram by Virco up to RT residue 400 and ViroSeq by Abbott/Celera Diagnostics up to RT residue 335).

The present study identifies N348I as a MDR mutation in HIV-1 RT. This knowledge provides information that may be useful in designing more efficient therapeutic strategies that can improve clinical outcome and help prevent the emergence of MDR variants, especially in salvage therapy. This work further highlights the functional role of the HIV-1 RT connection subdomain in drug resistance. Future studies that focus on the structural and biochemical properties of connection subdomain RT mutants should reveal the molecular details of NRTI and NNRTI drug resistance caused by connection subdomain residues.

ACKNOWLEDGMENTS

This work was supported by a grant for the promotion of AIDS Research from the Ministry of Health, Labor and Welfare (to A.H., E.K., Y.S., M.M., H.G., M.T., and S.O.), a grant for Research for Health Sciences Focusing on Drug Innovation from The Japan Health Sciences Foundation (E.K and M.M), a grant from the Organization of Pharmaceutical Safety and Research (A.H., H.G., and S.O.) and a grant from the ministry of Education, Culture, Sports, Science, and Technology (E.K).

We thank Yukiko Takahashi and Fujie Negishi for sample preparation and the AIDS Clinical Center coordinator nurses for their dedicated assistance.

REFERENCES

1. **Antinori, A., M. Zaccarelli, A. Cingolani, F. Forbici, M. G. Rizzo, M. P. Trotta, S. Di Giambenedetto, P. Narciso, A. Ammassari, E. Girardi, A. De Luca, and C. F. Perno.** 2002. Cross-resistance among nonnucleoside reverse transcriptase inhibitors limits recycling efavirenz after nevirapine failure. AIDS Res. Hum. Retrovir. **18**:835–838.
2. **Baldanti, F., S. Paolucci, G. Maga, N. Labo, U. Hubscher, A. Y. Skoblov, L. Victorova, S. Spadari, L. Minoli, and G. Gerna.** 2003. Nevirapine-selected mutations Y181I/C of HIV-1 reverse transcriptase confer cross-resistance to stavudine. AIDS **17**:1568–1570.
3. **Boyer, P. L., S. G. Sarafianos, E. Arnold, and S. H. Hughes.** 2002. Nucleoside analog resistance caused by insertions in the fingers of human immunodeficiency virus type 1 reverse transcriptase involves ATP-mediated excision. J. Virol. **76**:9143–9151.
4. **Brehm, J. H., D. Koontz, J. D. Meteer, V. Pathak, N. Sluis-Cremer, and J. W. Mellors.** 2007. Selection of mutations in the connection and RNase H domains of human immunodeficiency virus type 1 reverse transcriptase that increase resistance to 3′-azido-3′-dideoxythymidine. J. Virol. **81**:7852–7859.
5. **Brenner, B., D. Turner, M. Oliveira, D. Moisi, M. Detorio, M. Carobene, R. G. Marlink, J. Schapiro, M. Roger, and M. A. Wainberg.** 2003. A V106M mutation in HIV-1 clade C viruses exposed to efavirenz confers cross-resistance to non-nucleoside reverse transcriptase inhibitors. AIDS **17**:F1–5.
6. **Brown, A. J., H. M. Precious, J. M. Whitcomb, J. K. Wong, M. Quigg, W. Huang, E. S. Daar, R. T. D'Aquila, P. H. Keiser, E. Connick, N. S. Hellmann, C. J. Petropoulos, D. D. Richman, and S. J. Little.** 2000. Reduced susceptibility of human immunodeficiency virus type 1 (HIV-1) from patients with primary HIV infection to nonnucleoside reverse transcriptase inhibitors is associated with variation at novel amino acid sites. J. Virol. **74**:10269–10273.
7. **Caride, E., R. Brindeiro, K. Hertogs, B. Larder, P. Dehertogh, E. Machado, C. A. de Sa, W. A. Eyer-Silva, F. S. Sion, L. F. Passioni, J. A. Menezes, A. R. Calazans, and A. Tanuri.** 2000. Drug-resistant reverse transcriptase genotyping and phenotyping of B and non-B subtypes (F and A) of human immunodeficiency virus type I found in Brazilian patients failing HAART. Virology **275**:107–115.
8. **Cherrington, J. M., A. S. Mulato, M. D. Fuller, and M. S. Chen.** 1996. Novel mutation (K70E) in human immunodeficiency virus type 1 reverse transcriptase confers decreased susceptibility to 9-[2-(phosphonomethoxy)ethyl]adenine in vitro. Antimicrob. Agents Chemother. **40**:2212–2216.
9. **Das, K., S. G. Sarafianos, A. D. Clark, Jr., P. L. Boyer, S. H. Hughes, and E. Arnold.** 2007. Crystal structures of clinically relevant Lys103Asn/Tyr181Cys double mutant HIV-1 reverse transcriptase in complexes with ATP and non-nucleoside inhibitor HBY 097. J. Mol. Biol. **365**:77–89.
10. **de Jong, J. J., J. Goudsmit, V. V. Lukashov, M. E. Hillebrand, E. Baan, R. Huismans, S. A. Danner, J. H. ten Veen, F. de Wolf, and S. Jurriaans.** 1999.